DOE/NASA/51040-55
NASA TM-83676

NASA-TM-83676
19840017725

Creep-Rupture Behavior of Candidate Stirling Engine Alloys after Long-Term Aging at 760° C in Low-Pressure Hydrogen

Robert H. Titran
National Aeronautics and Space Administration
Lewis Research Center

May 1984

Prepared for
U.S. DEPARTMENT OF ENERGY
Conservation and Renewable Energy
Office of Vehicle and Engine R&D

DISCLAIMER

Printed in the United States of America

Available from
National Technical Information Service
U.S. Department of Commerce
5285 Port Royal Road
Springfield, VA 22161

NTIS price codes[1]
Printed copy: A02
Microfiche copy: A01

[1]Codes are used for pricing all publications. The code is determined by the number of pages in the publication. Information pertaining to the pricing codes can be found in the current issues of the following publications, which are generally available in most libraries: *Energy Research Abstracts (ERA); Government Reports Announcements* and Index (*GRA* and I); *Scientific and Technical Abstract Reports (STAR);* and publication, NTIS-PR-360 available from NTIS at the above address.

DOE/NASA/50140-55
NASA TM-83676

Creep-Rupture Behavior of Candidate Stirling Engine Alloys after Long-Term Aging at 760° C in Low-Pressure Hydrogen

Robert H. Titran
National Aeronautics and Space Administration
Lewis Research Center
Cleveland, Ohio 44135

May 1984

Work performed for
U.S. DEPARTMENT OF ENERGY
Conservation and Renewable Energy
Office of Vehicle and Engine R&D
Washington, D.C. 20545
Under Interagency Agreement DE-AI01-77CS51040

CREEP-RUPTURE BEHAVIOR OF CANDIDATE STIRLING ENGINE ALLOYS AFTER LONG-TERM AGING AT 760° C IN LOW-PRESSURE HYDROGEN

Robert H. Titran
National Aeronautics and Space Administration
Lewis Research Center
Cleveland, Ohio 44135

SUMMARY

Candidate Stirling automotive engine heater head tube and cylinder-regenerator housing alloys were aged at 760° C for 3500 hr in a low pressure argon or hydrogen atmosphere to determine the resulting effects on mechanical behavior. The five candidate heater head tube alloys evaluated were CG-27, W545, 12RN72, INCONEL-718, and HS-188. The four candidate cylinder and regenerator housing alloys evaluated were SA-F11, CRM-6D, XF-818, and HS-31. Aging produced a slight refinement in alloy grain size possibly due to enhancement of previously unresolved precipitates. Aging promoted an increase in amount and size of precipitates in the grains, grain boundaries, and interdendritic spaces. Tensile properties were generally but not always degraded by aging. At 870° C the unaged to the H_2 aged (unaged/H_2 aged) 0.2 offset yield strengths are as follows: CG-27, 535/311 MPa; W545, 400/243 MPa; 12RN72, 124/124 MPa; INCONEL-718, 365/357 MPa; HS-188, 178/340 MPa; SA-F11, 428/438 MPa; CRM-6D, 349/331 MPa; XF-818, 318/249 MPa, and HS-31, 152/346 MPa. Aging also decreased creep-rupture strength but to a somewhat lesser extent. At 815° C the unaged to the H_2 aged (unaged/H_2 aged) 1000 hr rupture-life stress levels are: CG-27, 135/130 MPa; W545, 52/65 MPa; 12RN72, 48/46 MPa; INCONEL-718, 50/50 MPa; HS-188, 100/110 MPa; SA-F11, 130/115 MPa; CRM-6D, 110/100 MPa; XF-818, 115/95 MPa, and HS-31, 150/150 MPa. The presence of hydrogen during aging did not contribute significantly to creep strength degradation. Based on current MOD 1-A Stirling engine design criteria (55 percent urban - 45 percent highway driving cycle); CG-27 was the only iron-base tube alloy with adequate 870° C rupture-strength while all three iron-base alloys, SA-F11, CRM-6D, and XF-818, for cast cylinders and regenerator housings had adequate 775° C strength.

INTRODUCTION

The Stirling Engine is under investigation in the DOE/NASA Stirling Engine Highway Vehicle Systems Program (ref. 1) as an alternative to the internal combustion engine for automotive applications. The work described in this report is a continuation of a supporting materials research and technology program under way at NASA Lewis Research Center (ref. 2). The Stirling Engine heater head, which consists of the cylinders, tubing, and regenerator housings, has been assessed as the most critical materials component (ref. 3). The major high temperature materials requirement and the current state-of-the-art of metals and ceramics are described in recent assessments of Stirling engine materials technology (refs. 4 to 6). A schematic representation of a prototype automotive Stirling engine is shown in figure 1.

In the automotive Stirling engine, the thermodynamic working fluid, hydrogen, is passed through a hot zone, created from combustion gases, in a series of thin-wall tubes (4.5 mm o.d. x 3 mm i.d.). The high pressure gas is expanded to drive one or more pistons, which actuate the drive system. The gas

is cooled by passing it through a regenerator and cooler. The hydrogen working fluid is then recirculated back to the hot zone to repeat the cycle. Loss of hydrogen by rupture in either the tubing or the cylinder results in loss of the engine power system. One of the major design criteria of heater head materials becomes their creep-rupture behavior.

Candidate heater-head materials for commercial Stirling engines are expected to meet such requirements as high temperature strength, compatability with hydrogen, resistance to hydrogen permeation, oxidation resistance, and be of low cost. The planned automotive application requires a cyclic on-off operation of 161 000 km (100 000 mile) with resulting temperatures in the heater-head ranging from ambient to near 900° C (ref. 5). In addition, speed of the automobile is controlled by pressure variations of the hydrogen working fluid contained in the heater-head tubing and cylinders. Based on a 55 percent urban/45 percent highway driving cycle, pressure will normally range between 2 and 15 MPa with an average pressure near 7 MPa. It has been calculated that the 161 000 km engine life will be equivalent to a driving time of 3500 hr at the average pressure of 7 MPa.

The purpose of this study was to evaluate and rank a second series of candidate alloys for both the heater-head tubes and the cylinders and regenerator housings. An initial series of alloys was previously evaluated (ref. 2) under similar conditions. Current prototype automotive Stirling engines utilize the cobalt base alloy HS-31 and the N-155 alloy, an alloy containing 20 percent cobalt, in the heater head. Because of the limited production and availability of cobalt and its cost, it is not practical to consider cobalt containing alloys for the automotive application of the Stirling engine. Due to the increased temperature requirements, it was determined that a second series of iron-base alloy should be evaluated since those examined previously (ref. 2) would or could not meet the anticipated engine requirements. The cobalt-base alloys, HS-188 and HS-31 were included in this study for comparative purposes.

The evaluation reported herein examined changes in the mechanical properties, particularly creep-rupture behavior in air, as a result of long term exposure to low pressure hydrogen (H_2) at 760° C (near the maximum temperature anticipated in earlier versions of the Stirling automotive engine). To discern the effect of hydrogen, aging in low pressure argon (Ar) atmosphere was also investigated. The mechanical behavior of nine commercially available alloys was evaluated before and after long term (3500 hr) aging at 760° C in argon and in H_2 atmospheres. Tensile properties determined at 25°, 425°, and 760° C are presented. Creep-rupture properties determined over a temperature range of 650° to 925° C are presented for the unaged material. Creep-rupture data for the argon and hydrogen aged materials tested at 760° and 815° C are compared with the unaged data.

EXPERIMENTAL DATA

Composition of the nine candidate heater-head alloys used in this investigation are listed in table I. All candidate tubing alloys were evaluated in the form of sheet material which ranged in thickness from 0.69 to 0.94 mm. Creep-rupture specimens, with a reduced gage section of 9.5 mm wide by 31.8 mm long, as shown in figure 2(a), were die stamped from available sheet. All candidate cylinder and regenerator housings alloys were evaluated in the form

of investment castings. Creep-rupture test specimens were cast with gating through the ends, which resulted in a reduced gage section diameter of 6.35 mm by 31.8 mm long, as shown in figure 2(b). Table II lists the heat treatment for each alloy that resulted in the "unaged" condition.

Long term aging of the test specimens was conducted in cylindrical stainless steel chambers heated by external resistance element furnaces. The aging treatments were conducted at 760°±15° C for 3500 hr. Flowing argon or hydrogen atmospheres were maintained in the chambers at a gage pressure of 30 to 60 kPa. Commercial high purity hydrogen, having typically a dew point of -65° C and containing 45 ppm oxygen and 1100 ppm nitrogen, was passed through a palladium purifier prior to entering the aging chamber. The commercial high purity argon was not treated prior to entry of the aging chamber.

Tensile and creep-rupture tests were conducted in air. Tensile properties were determined at room temperature, 425° C and 760° C at a crosshead speed of 1.2 mm/min. Constant load creep-rupture tests conforming to ASTM E-139 were conducted at 650°, 705°, 760°, 815°, 870°, and 925° C in conventional beam-loaded machines. Creep strain measurements were determined from the movement of an extensometer attached to the reduced section of the specimens and converted to an electrical signal by means of a linear variable differential transformer. Test temperatures were measured by Pt/Pt-13 percent Rh thermocouples attached to the specimen reduced section.

The longitudinal microstructure of each of the candidate alloys in the unaged and long term aged conditions were studied by light microscopy. The average grain sizes for the alloy sheet materials were determined using the circle intercept (50-cm-diam) method. Tensile fracture surfaces were examined with a scanning electron microscope (SEM).

RESULTS AND DISCUSSION

Microstructure

The iron-base alloys were tested in three conditions: unaged, Ar aged, and H_2 aged. The unaged condition resulted from the heat treatment listed for each alloy in table II. The Ar aged and H_2 aged conditions resulted from exposure of the unaged alloy structure to a temperature of 760° C for 3500 hr in an atmosphere of Ar or H_2. Hydrogen analysis of the alloys before and after H_2 aging given in table III indicated all alloys except the cobalt base alloys H-31 and HS-188, increased in hydrogen content. For example, the H_2 aging treatment increased the H_2 content in CG-27 from 1.2 to 11.4 ppm. (The lack of an increase in hydrogen content for HS-31 and HS-188 is similar to that found previously for the N-155 alloy (ref. 2). It is of interest to note that these three alloys are the cobalt-bearing alloys, with nominally 55, 40, and 20 wt.%, respectively.) It is further shown in table III that, after air creep testing, H_2 content decreases apparently due to H_2 diffusion out of the specimen. The heat-treated hardness of the wrought and cast alloys are given in table IV. Generally, few major changes in hardness were noted, the exceptions being INCONEL-718 and HS-188 which show increases in hardness values by 15 and 9, respectively, due to the H_2 aging cycle.

A microstructural analysis was made of all the alloys in the unaged and aged condition prior to creep-rupture testing. The microstructures of the 5

wrought (tubing) alloys in the unaged condition are shown in figures 3(a) to (e). All the wrought alloys showed fully austenitic microstructure with varying degrees of twinning and varying amounts of second phase particles. It is believed that the bulk of the particles are undissolved carbides and nitrides. The average grain size of the CG-27 alloys was 158.9 μm, the largest for any of the wrought alloys tested as shown in table V. Accompanying this large grain size, CG-27 also has the highest room temperature hardness, 61 Rockwell 30N, as shown in table IV.

The microstructure of the 4 cast alloys in the unaged condition is shown in figures 4(a) to (d). The structures clearly indicate the discrete precipitates constituting the dendrite walls, and some coring effect is noted in CRM-6D and SA-F11. In HS-31, the structural continuity at the boundaries is much less evident and only traces of lamellar structure are noted. The hardness values of the cast alloys fell into a rather narrow range, 56 (for the CRM-6D and HS-31) to 43 (for XF-818) as shown in table IV.

Typical microstructures for an aged wrought alloy and an aged cast alloy are illustrated in figures 5 and 6. Figure 5 shows the resultant microstructure following a 3500 hr aging treatment at 760° C for CG-27. Extensive precipitation has taken place with a continuous grain boundary carbide network accompanied by an adjacent denuded zone. This microstructure was also typical for the W545, INCONEL-718, and 12RN72 alloys regardless of aging atmosphere. After aging, an approximate 50 percent reduction in the average grain size of W545 and CG-27 was noted, see table V. It is believed that the grain boundaries prior to the 3500 hr 760° C aging for these alloys were very clean and essentially unresolved. After aging these unresolved grain boundaries become highly decorated with precipitates. The INCONEL-718 and HS-188 tended to age harden slightly based upon the hardness values of table IV, while the remaining wrought alloys essentially overaged with little change in hardness. Figure 6 shows the resultant microstructure following 3500 hr 760° C aging treatment for the cast alloy XF-818. Extensive precipitation within the dendrites has taken place and there is a tendency to coarsen the lamellar M_3B_2 + carbide phase along with the interdendritic carbides.

The same trend was noted for the SA-F11 and CRM-6D alloys, but to a lesser degree for each, presumably due to the decreasing boron content with an accompanying increase in carbon content in these alloys. Long term aging had no effect on hardness values as shown in table IV.

Tensile Behavior

The tensile properties of the candidate heater tube alloys at 25°, 425°, and 760° C in the unaged and aged condition are presented in table VI. As shown in figure 7(a), two of the tubing alloys, W545 and CG-27, both had losses in ultimate strength of approximately 25 percent as a result of the aging treatment. The effect of aging on the yield strength was considerably less for all alloys. All alloys except 12RN72 showed extensive loss of ductility due to aging as shown in figure 7(B). At 760° C the tensile strength behavior of the tubing alloys was similar to the 25° C data. The tensile data for the tubing alloys indicate that the aging treatment itself has an adverse affect on yield strength, however, the hydrogen atmosphere was no more severe than the argon atmosphere. As shown in figure 7(d), aging generally resulted in a substantial increase in tensile ductility at 760° C. Changes in tensile ductility (percent elongation) in response to aging varied with each alloy and

test temperature. At 25° C the CG-27 alloy had a 90 percent reduction in ductility, the remaining alloys also showed a loss of ductility but to a lesser extent. However, at 760° C, 4 of the 5 tube alloys showed increases in ductility ranging from 50 percent for CG-27 to 90 percent for 12RN72. The exception was INCONEL-718 which exhibited a loss in ductility of 40 percent after aging.

The tensile properties of the candidate cylinder and regenerator housing alloys at 25°, 425°, and 760° C in the unaged and aged condition are presented in table VII. As shown in figures 8(a) and (d) the three iron base cast alloys had different responses to the aging treatment in regard to room temperature and 760° C tensile strength. The increases and losses were not very large, averaging about 15 percent. However, changes in room temperature and 760° tensile ductility (percent elongation), shown in figures 8(b) and (d), although as varied in response to aging as was the strength data, showed that the XF-818 had a beneficial response to the 3500 hr aging treatment. Tensile elongation increased 2 to 3 fold over the unaged condition. Again the data indicate that the aging treatment itself had a more pronounced effect on tensile behavior than either an argon or hydrogen environment.

A fractographic study of all the alloys was conducted by Scanning Electron Microscopy (SEM) on unaged, Ar aged, and H_2 aged room temperature tensile specimens. For brevity a description of a wrought and a cast alloy in the unaged and H_2 aged condition is presented.

Fracture surface examination of the CG-27 alloy revealed the ductile nature of the unaged room temperature tensile specimen as indicated by the extensive dimpling in figure 9(a); the hydrogen aged condition in figure 9(b) showed very little dimpling and failed intergranularly with some transgranular cleavage. Particles 1 to 5 μm in diameter were noted among the dimples of the unaged condition. The aged condition had numerous particles in excess of 10 μm on the cleaved surfaces. The decrease in ductility (measured as percent elongation) in CG-27 is due to the extensive precipitation and coarsening of particles at grain boundaries resulting from the aging cycle and not the environment. Fracture surface examination of the XF-818 alloy revealed the effects of thermal aging on improving the ductility (figs. 10(a) and (b)). It is believed that the extensive formation of the finely spaced lamellar M_3B_2 (fig. 10(b)) contributed to the ductility increase in aged XF-818.

Creep-Rupture Behavior

Base line creep-rupture data obtained from tests of the unaged alloys at 650° to 925° C as well as results from similar tests on aged materials at 760° and 815° C are summarized in table VIII. The effects of stress on the minimum creep rates and on the rupture lives for unaged alloys at 760° and 815° C are presented in figures 11 and 12. For comparison, the creep-rupture results for the Ar and H_2 aged specimens are included in these figures.

Using multiple linear regression analysis, apparent activation energies for creep were determined for each alloy in the unaged condition based on minimum creep rates as well as rupture lives. These apparent activation energy values are listed in table IX along with stress exponents and constants for the following relationships:

$$\ln \dot{\varepsilon}_m = \ln K_1 + n_1 \ln \sigma_1 + Q_1/RT \quad (1)$$

$$\ln t_r = \ln K_2 + n_2 \ln \sigma_2 + Q_2/RT \quad (2)$$

where $\dot{\varepsilon}_m$ is the minimum creep rate (sec^{-1}), t_r is rupture life (hr), K_1 and and K_2 are material constants, n_1 and n_2 are stress-term exponents, σ is stress (MPa), R is the gas constant (8.314 J/K-mol), T is absolute temperature (K), and Q_1 and Q_2 are the apparent activation energies for creep (J/mol) (refs. 8 to 10). Equations (1) and (2) along with the values of the parameters in table IX are useful in interpolation of rupture lives and minimum creep rates within the present test conditions. Thus a high degree of reliability is placed in the stress levels calculated for the candidate alloys 3500 hr rupture lives.

It is noted in figure 11 that all of the candidate tubing alloys except 12RN72 are plotted with two slopes for minimum creep rate ($\dot{\varepsilon}_m$) versus stress (σ). Each slope represents the best fit for a given stress region and the change in slope suggests a change in creep mechanism. The minimum creep rate ($\dot{\varepsilon}_m$) equation for each slope is given by table IX by the coefficient (Q_1, n_1, and $\ln K_1$) and is valid for the stress range given. The HS-188, CG-27, and 12RN72 alloys likewise exhibited two separate slopes for rupture life (t_r) versus stress (σ) and have distinct stress regions. The stress regions along with determined rupture life behavior coefficients are indicated in table IX.

From figure 12 and table IX it is noted that the minimum creep rate behavior of XF-818 and HS-31, as a function of stress and temperature, are best described by two equations. XF-818 is the only cast alloy studied whose rupture life is described by equations for two distinct stress regions.

In showing the creep-rupture behavior of the aged materials in figures 11 and 12 an initial assumption was made that long term aging resulted in creep properties that were displaced from but paralleled those of the unaged alloy. This would imply that microstructural changes due to the aging treatment would not alter the apparent activation energy or stress exponent terms, but would change the value of the materials constant K in equations (1) and (2). Upon examination of the minimum creep rates and rupture lives versus stress data for HS-188, 12RN72, and HS-31 (figs. 11(d), (e) and (i), and 12(d), (e), and (i) the above assumption appears quite valid and acceptable. However, heat treatment changes, such as precipitate morphology, precipitate density and grain boundary characteristics did affect the remaining alloys. Wherever possible, the parallelism between the unaged and aged creep-rupture properties was maintained in figures 11 and 12.

The effects of long term aging on creep strength is further illustrated in figure 13, which shows gains or losses in the 1000 hr rupture strength due to aging in argon or hydrogen for test temperatures of 760° and 815° C. It is apparent that aging per se is detrimental to the creep strength of the iron-base alloys at 760° C and that the presence of hydrogen during aging contributed further to the degradation of W545 and CG-27. However, at 815° C, W545 gained in strength after aging and in hydrogen and argon. In the case of the tubing alloys, the results of creep testing at 815° C suggests that the effects of the environmental aging cycle is less at elevated temperatures.However, at 815° C, W545 gained in strength after aging and in hydrogen and argon. In the

case of the tubing alloys, the results of creep testing at 815° C suggests that the effects of the environmental aging cycle is less at elevated temperatures. It has not been determined whether or not a grain size effect exists with this group of alloys. The W545 and INCONEL-718 alloys which show the greatest and comparable degradation at 760° C and are at the extremes in grain size (78 and 7 μm, respectively), suggesting the degradation may simply be a compositional effect.

Elongation measurements following rupture generally indicated decreased ductility with increased stress at constant temperature, over the range of loads applied to unaged alloys in this study. In the case of CG-27, the unaged ductility (percent elongation) remained fairly constant, about 3 percent at 760° C and 10 percent at 815° C, over the range of stresses studied. However the aged CG-27 showed ductilities of 25 percent at 760° C and 10 percent at 815° C. The aged CG-27 generally showed higher creep rates, higher ductility and shorter rupture lives than the unaged CG-27 tested at comparable stresses. The unaged XF-818 alloy shows a relatively uniform elongation of 14 percent at 760° C and 815° C for the stress range studied. Aging does not appear to have any adverse effect on the percent elongation of XF-818. Aging does appear to improve the reduction-in-area of XF-818 which in turn leads one to believe that the elevated temperature fatigue life should improve also.

The apparent effect of long term aging on the iron-base superalloys was to increase rupture ductility along with an increase in creep rate and therefore a resultant decrease in rupture life.

Engine Requirement and Alloy Selection

The design criteria for the MOD 1A Stirling automotive engine at startup require a maximum yield stress in the heater head tubes of 102 MPa at the operation temperature (ref. 10). All the alloys studied exhibited yield strengths in excess of 102 MPa in the unaged condition at 760° C. Although aging did reduce significantly the yield strengths of W545 and CG-27, their 760° C yield strength after aging did exceed the design criterion by a factor greater than 2 (see table VI).

The design criteria presently applied to the cylinder and regenerator housings show that for maximum pressurization (20 MPa) and associated thermal gradients static stress levels of 125 MPa in the cylinder housing and 280 MPa in the regenerator housing are to be expected. The 760° C unaged yield strengths of the cast iron-base superalloys exceeds the design criteria for both components. However, the calculated design stress levels in the regenerator housing exceed that of the hydrogen aged yield strengths of CRM-6D and XF-818 at 760° C (see table VII).

The MOD 1A Stirling automotive engine design criteria is based upon 3500 hr of engine operation under a combined 55 percent urban/45 percent highway driving cycle. The heater head tubes will experience a mean temperature of 820° C and the cylinder-regenerator housings a maximum temperature of 775° C. The hydrogen working fluid will have an equivalent average pressure of 7.2 MPa. The design criteria include a safety factor of 1.5; thus the design stress needed for a target rupture life of 3500 hr would be about 28 MPa for heater head tubes and 119 MPa for cylinder housings. The mean heater head tube temperature 820° C is based on a 870° C combustor flame side and 770° C tube back

side temperature profile. Therefore, the heater head tube alloys in the MOD 1A engine must have rupture lives of at least 3500 hr for a stress of 28 MPa at 870° C and the cylinder/regenerator housing cast alloys must have lives of at least 3500 hr for a stress of 119 MPa at 775° C.

In figure 14(a) the temperature dependence is shown for extrapolated 3500 hr rupture strength of the candidate heater head tube alloys in this study. CG-27 is the only unaged iron-base alloy which satisfies the MOD 1A engine requirements. If we assume that aging of the heater tube will occur in a manner similar to that of this study and that a parallel reduction in strength is similar to that noted at 760° and 815° C, the CG-27 alloy appears highly acceptable. In figure 14(b) the temperature dependence is shown for extrapolated 3500 hr rupture strengths of the candidate cast cylinder/ regenerator housing alloys in this study. In the unaged condition all three cast iron-base alloys exceed the MOD 1A engine long term requirements. If we again assume similar aging and strength reductions noted in the 760° C creep-rupture data, then XF-818 and CRM-6D and SA-F11 are considered acceptable alloys.

CONCLUDING REMARKS

This study has shown that long term aging generally degrades the tensile and creep-rupture properties of candidate iron-base Stirling engine alloys and is consistent with previous studies of Witzke and Stephens (ref. 2). The CG-27 alloy appears to have the best potential of the heater tube alloys and the cylinder/regenerator housing alloys XF-818, CRM-6D, and SA-F11 meet the current design requirements int the MOD 1A Stirling automotive engine criteria. Modifications in alloy composition as well as heat treatment to improve or optimize creep-rupture strength, fatigue, corrosion, and oxidation resistance are currently being investigated.

CONCLUSION

Based on the mechanical behavior of the candidate Stirling engine iron-base alloys evaluated before and after aging for 3500 hr at 760° C, the following was concluded:

1. CG-27, XF-818, CRM-6D, and SA-F11 are the only iron-base alloys in this study with adequate rupture strength to meet the design criteria of the MOD 1A Stirling automotive engine.

2. Aging per se reduces creep-rupture strength of the iron-base alloys. The presence of hydrogen during aging does not significantly affect the creep-rupture strength.

3. Changes in tensile ductility and yield strength occur as a result of long term aging, but hydrogen and argon aging atmospheres generally do not produce appreciably different tensile properties.

REFERENCES

1. Brogan, J. J.: Highway Vehicle Systems Program Overview. Highway Vehicle Systems, CONF-771037, U.S. Department of Energy, 1978, pp. 3-5.

2. Witzke, W. R.; and Stephens, J. R.: Creep-Rupture Behavior of Seven Iron-Base Alloys after Long Term Aging at 760° C in Low Pressure Hydrogen. NASA TM-81534, 1980.

3. Stephens, J. R.; et al.: Materials Technology Assessment for Stirling Engines. CONS/1011-22, NASA TM-73789, 1977.

4. Stephens, J. R.; Cronin, M. T.; and Skog, E.: Stirling Engine Materials Research at NASA Lewis, MTI a USAB. Proceedings of the Twentieth Automotive Technology Development Contractors' Coordination Meeting, P-120, Society of Automotive Engineers, Apr. 1983, pp. 103-113.

5. Tomazic, W. A.: A Look at a Cooled Insulated Stirling Engine Proceedings of the Twentieth Automotive Technology Development Contractors' Coordination meeting, P-120, Society of Automotive Engineers, Apr. 1983. pp. 131-141.

6. Gronwall, J.: Tentative Heater Design Stress Criteria in Automotive Application. Report 81-0023, United Stirling Feb. 82.

7. Ragsdale, R. G.: Stirling Engine Project Status. Proceedings of Highway Vehicle Systems, CONF-781050, U.S. Department of Energy, 1979, pp. 287-291.

8. Garofalo, Frank: Fundamentals of Creep and Creep-Rupture in Metals. MacMillian Co., 1965.

9. Sherby, O. D., and Burke, P. M.: Mechanical Behavior of Crystalline Solids at Elevated Temperature. Progress in Materials Science, B. Chalmers and W. Hume - Rothery, eds., Pergamon Press, Vol. 13, No. 7, 1967.

10. Conway, Joseph B.: Numerical Methods for Creep and Rupture Analyses. Gordon and Breach, 1967.

TABLE I. - COMPOSITION OF CANDIDATE STIRLING ENGINE HEATER-HEAD ALLOYS

Alloy	Element, percent by weight													
	Fe	Cr	Ni	Co	Mn	Si	W	Mo	Nb/Ta	Al	Ti	C	N	Other
W545	Bal	12.9	27.7	----	1.32	0.49	----	1.7	----	0.15	2.8	0.026	----	0.048B
INCONEL-718	18.0	18.6	Bal	0.12	.17	.19	----	3.1	5.3	.41	.74	.04	----	------
CG-27	Bal	13.0	37.8	----	----	.1	----	5.57	.97	1.66	2.3	.04	----	.004B
12RN72	Bal	18.8	25.2	----	1.75	.30	----	1.5	----	----	.49	.088	0.016	.01B
HS-188	1.35	22.0	23.3	Bal	.62	.45	14.4	----	----	----	----	.07	----	.004B .08La
SA-F11	Bal	23.0	15.6	----	.65	.68	11.9	----	----	----	----	.62	.039	.49B
CRM-6D	Bal	21.9	5.2	----	4.95	.38	.98	1.07	1.27	----	----	1.38	.048	.007B
XF-818	Bal	17.7	18.8	----	.18	.48	----	7.5	.50	----	----	.20	.11	1.08B
HS-31	1.67	25.1	10.4	Bal	.43	.47	7.4	----	----	----	----	.48	----	------

TABLE II. HEAT TREATMENT OF CANDIDATE STIRLING ENGINE HEATER-HEAD ALLOYS

Alloy	Thickness, mm	Heat treatment ("unaged" condition)
W545	0.94	Sol'n. ann. 1150° C/10 min in vac/fast furnace cool
INCONEL-718	.88	Sol'n. ann. 975° C/rapid cool. Age 715° C/8 hr/cool to 620° C/hold 8 hr.
CG-27	.69	Sol'n. ann. 1150° C/10 min in vac/fast furnace cool. age 760° C/16 hr in vac/cool to 650° C/hold 24 hr/ fast furnace cool
12RN72	.94	Sol'n. ann. 1175° C/15 min in vac/water quench
HS-188	.89	Sol'n. ann. 1150° C/15 min in vac/water quench
SA-F11	6.35	Sol'n. ann. 900° C/20 hr in vac/fast furnace cool
CRM-6D	6.35	Anneal 650° C/100 hr in vac/fast furnace cool
XF-818	6.35	None specified (as-cast)
HS-31	6.35	Anneal 730° C/50 hr in vac/fast furnace cool

TABLE III. - HYDROGEN ANALYSIS OF CANDIDATE STIRLING ENGINE HEATER-HEAD ALLOYS

Alloy	Hydrogen content, ppm by weight		
	Before aging	After 3500 hr at 760° C hydrogen (30 to 60 kPa gage)	
		Before creep testing	After creep testing
W545	3.1	8.6	4.7
INCONEL-718	2.9	7.2	2.5
CG-27	1.2	11.4	2.2
12RN72	5.0	9.7	1.6
HS-188	4.5	4.7	2.9
SA-F11	1.0	3.3	1.3
CRM-6D	5.7	9.2	8.0
XF-818	1.9	3.8	1.1
HS-31	6.4	6.0	3.7

TABLE IV. - HARDNESS DETERMINATIONS OF THE HEAT-TREATED AND AGED ALLOYS PRIOR TO CREEP-RUPTURE TESTING

Alloy	Hardness, Rockwell 30N (Brale) Scale					
	Unaged		Aged H_2		Aged Ar	
	Average	Range	Average	Range	Average	Range
W545	45	45 to 46	39	38 to 40	49	48 to 51
INCONEL-718	37	36 to 38	53	52 to 54	52	51 to 53
CG-27	61	60 to 63	58	58 to 59	60	59 to 61
12RN72	[a]70	[a]69 to 71	[a]71	[a]70 to 72	[a]71	[a]70 to 73
HS-188	43	43	52	51 to 53	49	49
SA-F11	49	47 to 51	54	54 to 55	50	50 to 53
CRM-6D	56	55 to 57	57	56 to 58	57	55 to 58
XF-818	43	43	45	45 to 46	44	42 to 45
HS-31	56	55 to 57	59	58 to 60	59	58 to 61

[a]12RN72 hardness numbers are Rockwell 30T (1/16 ball) scale.

TABLE V. - GRAIN SIZE MEASUREMENTS OF CANDIDATE HEATER TUBE ALLOYS

Alloy	Average grain diameter, μm, prior to testing in the following conditions		
	Unaged	Aged in Ar	Aged in H2
W545	99.7	64.6	78.4
INCONEL-718	9.1	8.0	6.8
CG-27	158.9	103.2	107.9
12RN72	44.0	45.3	47.6
HS-188	20.6	20.1	18.0

TABLE VI. - TENSILE PROPERTIES OF CANDIDATE HEATER HEAD TUBE ALLOYS

Alloy	Condition	25° C			425° C			870° C		
		YS, MPa	UTS, MPa	Elongation, percent[a]	YS, MPa	UTS, MPa	Elongation, percent[a]	YS, MPa	UTS, MPa	Elongation, percent[a]
W545	Unaged	475	959	[b]26	435	800	28	400	490	6
	Ar aged	407	790	[b]10	383	720	10	272	375	17
	H_2 aged	345	717	13	270	605	[b]10	214	346	26
INCONEL-718	Unaged	465	1005	50	308	705	[b]35	365	456	49
	Ar aged	615	1003	15	480	870	12	358	465	31
	H_2 aged	579	980	18	517	910	14	355	485	30
CG-27	Unaged	715	1290	15	685	1160	8	535	766	16
	Ar aged	628	1065	[b]2	570	1048	8	310	518	19
	H_2 aged	575	952	[b]3	490	----	[b]----	312	520	24
12RN72	Unaged	222	586	41	152	503	27	124	275	32
	Ar aged	202	585	34	159	448	22	124	228	50
	H_2 aged	191	568	36	145	469	24	127	215	59
HS-188	Unaged	438	965	57	248	607	[b]30	178	300	12
	Ar aged	483	915	8	375	747	[b]11	359	620	[b]38
	H_2 aged	505	1005	[b]13	---	-----	-----	320	550	52

[a]In 2.54 cm gage length.
[b]Broke at or outside gage mark.

TABLE VII. - TENSILE PROPERTIES OF CANDIDATE CYLINDER AND REGENERATOR HOUSING ALLOYS

Alloy	Condition	25° C				425° C				760° C			
		YS, MPa	UTS, MPa	Elongation, percent[a]	Reduction in area, percent	YS, MPa	UTS, MPa	Elongation, percent[a]	Reduction in area, percent	YS, MPa	UTS, MPa	Elongation, percent[a]	Reduction in area, percent
SA-F11	Unaged	---	[c]594	0	1	455	565	0	1	428	525	0	1
	Ar aged	---	[c]504	0	0	---	[c]487	0	0	441	509	2	2
	H_2 aged	---	[c]569	--[b]	-	---	[c]469	1	0	435	519	--[b]	--[b]
CRM-6D	Unaged	---	[c]579	1	1	489	[c]576	2	1	349	465	9	5
	Ar aged	---	[c]652	--[b]	-	475	[c]517	0	0	335	435	5	5
	H_2 aged	---	[c]530	1	1	447	[c]551	1	1	228	390	7	12
XF-818	Unaged	435	599	1	1	372	515	4	1	318	442	5	1
	Ar aged	472	661	4	2	472	661	4	2	246	415	10	12
	H_2 aged	424	638	3	2	284	514	4	3	249	407	8	10
HS-31	Unaged	305	373	2	4	218	376	6	4	152	276	20	25
	Ar aged	717	855	0	1	603	[c]703	0	1	380	590	4	5
	H_2 aged	617	634	2	1	558	[c]697	2	1	346	565	5	5

[a]In 2.54 cm gage length.
[b]Broke at or outside gage mark.
[c]Fracture strength.

TABLE VIII. - CREEP RUPTURE DATA

(a) W545

Condition	Test temperature, °C	Stress, MPa	Minimum creep rate, sec^{-1}	Rupture life, hr	Elongation to rupture, percent	Reduction in area, percent
Unaged	705	414	7.06×10^{-8}	49.9	6	--
		345	3.38×10^{-9}	228.0	6	--
		276	2.24×10^{-9}	811.8	5	--
	760	414	2.28×10^{-6}	1.9	5	--
		276	1.14×10^{-7}	64.8	15	--
		207	1.67×10^{-8}	223.7	10	--
		138	----------	807.3	8	--
	815	207	1.31×10^{-6}	12.3	11	--
		138	8.00×10^{-8}	43.4	13	--
		103	2.53×10^{-8}	127.6	19	--
		69	1.12×10^{-8}	303.0	17	--
		55	6.79×10^{-9}	------	--	--
		55	7.52×10^{-9}	1048.9	19	--
		41	6.77×10^{-9}	1915.8	29	--
	870	138	3.01×10^{-5}	1.5	31	--
		69	2.02×10^{-7}	46.3	23	--
		34	2.18×10^{-8}	910.1	25	--
	925	34	8.29×10^{-6}	11.5	68	--
		21	2.27×10^{-6}	91.8	--	--
Ar aged	760	207	1.43×10^{-6}	13.7	12	--
		138	4.03×10^{-8}	425.4	8	--
	815	138	9.33×10^{-7}	15.4	8	--
		103	8.12×10^{-8}	13.0	8	--
		69	1.06×10^{-8}	865.5	3	--
H_2 aged	760	138	1.48×10^{-7}	123.2	12	--
		103	1.04×10^{-8}	430.8	3	--
	815	138	2.04×10^{-6}	10.9	15	--
		103	3.26×10^{-7}	58.6	7	--
		69	1.12×10^{-8}	916.9	11	--

TABLE VIII. - CREEP RUPTURE DATA

(b) INCONEL-718

Condition	Test temperature, °C	Stress, MPa	Minimum creep rate, sec^{-1}	Rupture life, hr	Elongation to rupture, percent	Reduction in area, percent
Unaged	705	552	1.14×10^{-7}	33.5	31	--
		483	4.39×10^{-8}	85.8	27	--
		414	1.12×10^{-8}	(129.0)[a]	--	--
		345	7.81×10^{-9}	547.1	25	--
	760	414	6.17×10^{-7}	20.7	36	--
		276	1.02×10^{-7}	61.3	35	--
		207	2.96×10^{-8}	186.3	40	--
		172	2.12×10^{-8}	308.9	47	--
		138	8.41×10^{-9}	948.5	47	--
	815	207	3.54×10^{-7}	18.6	47	--
		207	2.53×10^{-7}	10.7	45	--
		138	1.51×10^{-7}	56.1	50	--
		103	1.06×10^{-7}	119.6	59	--
		69	3.57×10^{-8}	502.1	55	--
		55	4.00×10^{-8}	674.7	39	--
	870	103	2.08×10^{-6}	9.8	70	--
		69	4.33×10^{-7}	42.1	65	--
		55	2.94×10^{-7}	113.0	37	--
		34	7.92×10^{-8}	434.4	--	--
Ar aged	760	207	1.21×10^{-6}	24.8	52	--
		138	1.16×10^{-7}	246.0	55	--
	815	138	1.39×10^{-6}	(17.3)	--	--
		103	2.29×10^{-7}	79.6	78	--
		69	9.69×10^{-8}	390.9	82	--
H_2 aged	760	207	1.33×10^{-6}	22.9	82	--
		168	1.76×10^{-7}	157.4	55	--
		103	4.87×10^{-8}	616.0	52	--
	815	103	5.27×10^{-7}	(48.5)	--	--
		69	1.13×10^{-7}	305	52	--

[a]Data in parenthesis not used in multiple linear regression analysis due to test interruptions.

TABLE VIII. - CREEP RUPTURE DATA

(c) CG-27

Condition	Test temperature, °C	Stress, MPa	Minimum creep rate, sec^{-1}	Rupture life, hr	Elongation to rupture, percent	Reduction in area, percent
Unaged	705	483	2.30×10^{-8}	82.3	1	--
		414	4.78×10^{-9}	179.7	1	--
		414	1.35×10^{-8}	--------	--	--
	760	483	7.57×10^{-7}	4.5	5	--
		414	8.28×10^{-8}	19.7	3	--
		345	1.91×10^{-8}	81.1	2	--
		276	9.54×10^{-9}	339.6	4	--
		241	1.94×10^{-9}	--------	--	--
	815	483	8.38×10^{-5}	0.16	11	--
		345	8.29×10^{-7}	4.8	3	--
		276	8.41×10^{-8}	--------	--	--
		207	1.01×10^{-8}	126.3	6	--
		172	3.94×10^{-9}	--------	--	--
		138	2.45×10^{-9}	981.2	9	--
	870	276	6.42×10^{-6}	0.65	11	--
		241	1.68×10^{-6}	--------	--	--
		138	2.95×10^{-8}	52.7	9	--
		103	9.81×10^{-9}	150.0	7	--
	925	103	8.25×10^{-7}	3.6	25	--
		62	1.28×10^{-7}	77.7	24	--
Ar aged	760	345	5.85×10^{-6}	18.2	16	--
		276	5.88×10^{-7}	32.9	26	--
		241	--------	80	8	--
		207	1.44×10^{-8}	539.4	9	--
	815	207	8.00×10^{-7}	12.5	10	--
		138	2.30×10^{-9}	656.1	10	--
H_2 aged	760	345	(4.7×10^{-5})	18.9	21	--
		276	1.21×10^{-6}	21.8	29	--
		241	2.43×10^{-7}	(92)	9	--
		207	--------	(305)	(5)	--
	815	207	9.90×10^{-7}	14.8	13	--
		138	5.97×10^{-9}	603.6	6	--

TABLE VIII. - CREEP RUPTURE DATA

(d) 12RN72

Condition	Test temperature, °C	Stress, MPa	Minimum creep rate, sec^{-1}	Rupture life, hr	Elongation to rupture, percent	Reduction in area, percent
Unaged	650	207	2.57×10^{-8}	465	14	--
	705	172	1.81×10^{-7}	111.5	22	--
		138	4.33×10^{-8}	411.9	34	--
	760	207	9.48×10^{-5}	2.8	46	--
		117	3.00×10^{-7}	68.8	23	--
		83	3.6×10^{-8}	671.8	38	--
	815	83	1.38×10^{-6}	28.2	36	--
		69	7.42×10^{-7}	95.1	34	--
	870	69	4.03×10^{-6}	11.1	34	--
		38	5.13×10^{-8}	524.5	36	--
	925	28	3.88×10^{-8}	197	14	--
Ar aged	760	90	3.81×10^{-7}	216.4	57	--
		76	4.85×10^{-8}	1178.6	34	--
		69	3.89×10^{-8}	1408.7	28	--
	815	55	3.58×10^{-8}	235	(6)	--
		48	2.23×10^{-8}	744.7	(10)	--
		41	6.30×10^{-9}	3272.3	30	--
H_2 aged	760	90	5.98×10^{-7}	156.3	57	--
		76	1.46×10^{-7}	------	--	--
		76	1.13×10^{-7}	246.8	12	--
		69	5.21×10^{-8}	705	16	--
	815	55	7.37×10^{-8}	(346.6)	22	--
		48	4.89×10^{-8}	-------	(4)	--
		41	----------	1401.5	10	--

TABLE VIII. – CREEP RUPTURE DATA

(e) HS-188

Condition	Test temperature, °C	Stress, MPa	Minimum creep rate, sec^{-1}	Rupture life, hr	Elongation to rupture, percent	Reduction in area, percent
Unaged	650	448	2.42×10^{-7}	26.7	12	--
		414	1.12×10^{-7}	74.5	11	--
		345	6.24×10^{-9}	505.6	11	--
	705	414	4.39×10^{-6}	6.1	19	--
		276	7.43×10^{-8}	224.7	23	--
		221	2.32×10^{-8}	852.9	25	--
	760	276	---------	21.1	33	--
		276	3.62×10^{-6}	16.5	24	--
		221	5.44×10^{-7}	(82)	23	--
		172	1.22×10^{-7}	320.9	30	--
		138	4.00×10^{-8}	1444.4	26	--
	815	172	1.68×10^{-6}	43.7	42	--
		138	4.15×10^{-7}	19.5	35	--
		103	3.65×10^{-8}	958.8	27	--
	870	124	8.53×10^{-7}	21.5	32	--
		110	9.65×10^{-7}	54.6	40	--
		83	1.1×10^{-7}	266.1	28	--
		83	1.03×10^{-7}	380.6	23	--
	925	110	8.38×10^{-6}	5.9	45	--
Ar aged	760	221	7.08×10^{-7}	88.2	38	--
		172	9.2×10^{-8}	414.0	46	--
	815	138	2.01×10^{-7}	(127.2)	(22)	--
		103	2.05×10^{-8}	1055.1	40	--
H_2 aged	760	276	3.20×10^{-6}	19.2	67	--
		221	5.82×10^{-7}	92.1	68	--
		172	6.45×10^{-8}	582.7	45	--
	815	172	1.00×10^{-6}	53.4	56	--
		138	1.72×10^{-7}	216.0	50	--
		103	1.50×10^{-8}	1387.5	25	--

TABLE VIII. - CREEP RUPTURE DATA

(f) SA-F11

Condition	Test temperature, °C	Stress, MPa	Minimum creep rate, sec^{-1}	Rupture life, hr	Elongation to rupture, percent	Reduction in area, percent
Unaged	650	380	8.31×10^{-9}	269.9	5	2
	705	380	3.17×10^{-8}	7.3	5	4
		345	4.93×10^{-7}	197.7	6	8
	760	276	1.58×10^{-7}	48.1	6	6
		207	2.61×10^{-8}	224.5	7	17
		172	1.00×10^{-8}	1334.8	7	9
		152	3.00×10^{-9}	1686.5	5	5
	815	207	2.01×10^{-7}	41.4	4	7
		172	2.96×10^{-8}	199.8	6	5
		152	3.02×10^{-8}	258.2	10	15
		138	6.65×10^{-9}	640.7	2	5
	870	138	3.44×10^{-7}	31.3	19	34
		103	2.00×10^{-8}	473.7	10	24
		83	2.35×10^{-9}	1268.6	8	24
	925	83	5.31×10^{-8}	114.5	10	25
Ar aged	760	276	9.30×10^{-7}	8.1	6	9
		207	3.93×10^{-8}	151.6	5	5
		172	8.18×10^{-10}	1199.0	6	7
	815	172	7.10×10^{-8}	74.5	6	4
		138	1.02×10^{-8}	362.4	4	4
H_2 aged	760	276	9.20×10^{-7}	9.7	6	6
		241	(2.31×10^{-7})	28.8	5	7
		207	----------	184.4	4	4
	815	172	6.11×10^{-8}	86.0	3	6
		138	2.38×10^{-8}	217.8	5	5

TABLE VIII. - CREEP RUPTURE DATA

(g) CRM-6D

Condition	Test temperature, °C	Stress, MPa	Minimum creep rate, sec^{-1}	Rupture life, hr	Elongation to rupture, percent	Reduction in area, percent
Unaged	650	414	1.6×10^{-7}	52.2	6	8
	705	310	3.14×10^{-7}	50.3	9	13
		248	5.34×10^{-8}	(298)	13	29
		228	6.95×10^{-9}	1726.3	9	16
	760	248	----------	23.6	16	31
		228	4.27×10^{-7}	33.2	12	34
		207	1.63×10^{-7}	91.9	12	15
		172	3.03×10^{-8}	394.5	19	32
		172	9.22×10^{-9}	726.3	10	25
	815	186	1.88×10^{-6}	13.4	21	28
		166	1.28×10^{-6}	------	--	--
		138	9.18×10^{-8}	168.6	22	37
		103	2.34×10^{-9}	1883.7	10	15
	870	103	3.34×10^{-8}	192.1	11	16
		90	1.65×10^{-9}	720.1	6	11
	925	69	1.48×10^{-8}	289.1	10	28
Ar aged	760	207	5.92×10^{-7}	40.8	20	34
		172	9.23×10^{-8}	178.8	20	46
	815	186	5.82×10^{-6}	(4.5)	34	57
		172	(4.58×10^{-8})	(153.7)	13	32
		138	8.36×10^{-7}	20.5	16	41
H_2 aged	760	228	4.14×10^{-7}	32.7	14	30
		207	1.11×10^{-6}	(21.4)	20	42
		172	8.23×10^{-8}	154.0	14	41
	815	186	3.49×10^{-6}	5.1	14	13
		138	4.32×10^{-7}	49.5	30	60

TABLE VIII. - CREEP RUPTURE DATA

(h) XF-818

Condition	Test temperature, °C	Stress, MPa	Minimum creep rate, sec^{-1}	Rupture life, hr	Elongation to rupture, percent	Reduction in area, percent
Unaged	650	483	2.60×10^{-7}	7.9	6	12
		379	(6.7×10^{-9})	-------	2	4
		379	1.05×10^{-8}	813	8	7
	705	345	3.63×10^{-7}	18	3	16
		310	5.10×10^{-8}	128.2	6	12
		241	----------	2226.8	8	14
	760	276	6.08×10^{-7}	17.2	10	17
		207	8.74×10^{-8}	155.9	16	30
		172	3.58×10^{-9}	1348.0	14	13
	815	207	1.64×10^{-6}	6.6	17	31
		138	4.40×10^{-8}	198.6	13	43
		103	(3.21×10^{-9})	2263.0	10	18
		103	(1.12×10^{-8})	1346.9	18	22
	870	138	1.12×10^{-6}	14.8	13	31
		103	2.4×10^{-7}	83.0	18	25
		90	9.33×10^{-8}	189.0	20	25
	925	90	6.45×10^{-8}	31.7	22	25
		69	3.70×10^{-7}	139.9	16	38
Ar aged	760	241	1.53×10^{-6}	14.6	14	29
		207	1.94×10^{-7}	73.3	9	36
		172	8.55×10^{-8}	290.9	19	32
	815	172	8.52×10^{-7}	23.4	16	53
		138	1.508×10^{-9}	495.9	10	33
		103	4.23×10^{-9}	2583.0	18	35
H_2 aged	760	241	2.3×10^{-6}	10.5	17	31
		207	5.13×10^{-7}	37.3	15	45
		172	1.13×10^{-7}	215.5	18	39
	815	172	9.72×10^{-7}	14.5	13	53
		138	1.45×10^{-7}	113	13	42
		103	6.95×10^{-9}	2075.7	16	40

TABLE VIII. - CREEP RUPTURE DATA

(i) HS-31

Condition	Test temperature, °C	Stress, MPa	Minimum creep rate, sec^{-1}	Rupture life, hr	Elongation to rupture, percent	Reduction in area, percent
Unaged	650	345	5.20×10^{-8}	78.5	4	15
	705	345	5.33×10^{-7}	59.5	19	29
		290	1.81×10^{-7}	201.5	22	43
		248	6.53×10^{-8}	482.7	16	29
	760	290	3.42×10^{-6}	14.5	37	46
		207	3.56×10^{-8}	662.9	26	61
		172	2.39×10^{-8}	651.6	22	34
	815	386	----------	0.13	34	40
		290	(1.88×10^{-5})	2.1	22	50
		241	(4.67×10^{-6})	8.0	32	52
		172	2.38×10^{-7}	170.3	45	72
		152	1.10×10^{-8}	1059.5	30	66
	870	138	1.60×10^{-7}	109.8	26	63
		117	3.08×10^{-8}	322.9	14	31
		103	1.02×10^{-9}	------	--	--
	925	103	(4.6×10^{-10})	141.5	10	17
Ar aged	760	290	1.55×10^{-6}	20.7	26	49
		207	7.52×10^{-8}	397.7	24	69
	815	172	1.07×10^{-7}	216.4	34	60
		152	3.52×10^{-8}	317.8	25	68
H_2 aged	760	290	1.53×10^{-6}	18.2	26	51
		207	5.18×10^{-8}	601.6	30	65
	815	172	1.82×10^{-7}	160.2	47	72
		152	1.45×10^{-7}	1066.3	16	38

TABLE IX. - MULTIPLE LINEAR REGRESSION ANALYSIS OF CREEP AND RUPTURE LIFE OF UNAGED ALLOYS[a]

Alloy	Minimum creep rate data					Rupture life data				
	Stress range, MPa	Correlation coefficient, R^2	Q_1 kJ/mol	n_1	ln K_1	Stress range, MPa	R^2	Q_2 kJ/mol	n_2	ln K_2
W545	20 to 110	0.918	-687.08	1.61	50.63	20 to 350	0.914	478.97	- 3.46	-32.37
	130 to 420	.939	-778.79	7.66	32.29					
INCONEL-718	30 to 310	.940	-453.18	2.16	23.91	30 to 310	.982	442.96	-3.24	-29.07
	310 to 550	.976	-538.19	5.92	12.68	310 to 550	.998	337.36	-5.86	- 0.96
CG-27	60 to 140	.932	-643.09	2.72	37.31	60 to 140	.971	660.09	-4.85	-42.76
	170 to 500	.958	-580.38	9.08	-2.36	170 to 500	.971	492.60	-7.64	-8.71
12RN72	20 to 210	.961	-582.20	8.20	14.43	20 to 210	.970	405.73	-5.62	-16.39
HS-188	80 to 310	.964	-451.68	6.82	1.39	80 to 310	.986	409.15	-6.29	-9.44
	310 to 450	.997	-524.28	14.27	-33.79	310 to 450	.999	326.44	-11.09	28.45
SA-F11[b]	75 to 345	.951	-293.28	6.79	-19.48	75 to 345	.969	305.96	-6.18	3.84
CRM-6D	65 to 315	.904	-637.57	12.40	-7.36	65 to 315	.967	494.26	-8.77	-6.27
XF-818	5 to 175	.910	-534.57	7.39	6.05	5 to 175	.978	499.34	-6.79	-16.39
	175 to 380	.949	-565.59	10.48	-6.77	175 to 380	.969	561.79	-10.79	-2.53
HS-31[c]	100 to 210	.934	-834.04	18.24	-17.33	100 to 390	.925	330.57	-8.08	9.99
	240 to 345	.981	-384.19	7.07	-8.21					

[a]From equations (1) and (2) in text.
[b]Analysis of 760° and 815° C data only.
[c]$\dot{\varepsilon}_m$ data w/o 760° C - 172.4 MPa data pt; t_r data w/o 760° C - 172.4 MPa, and 650° C - 345 MPa data.

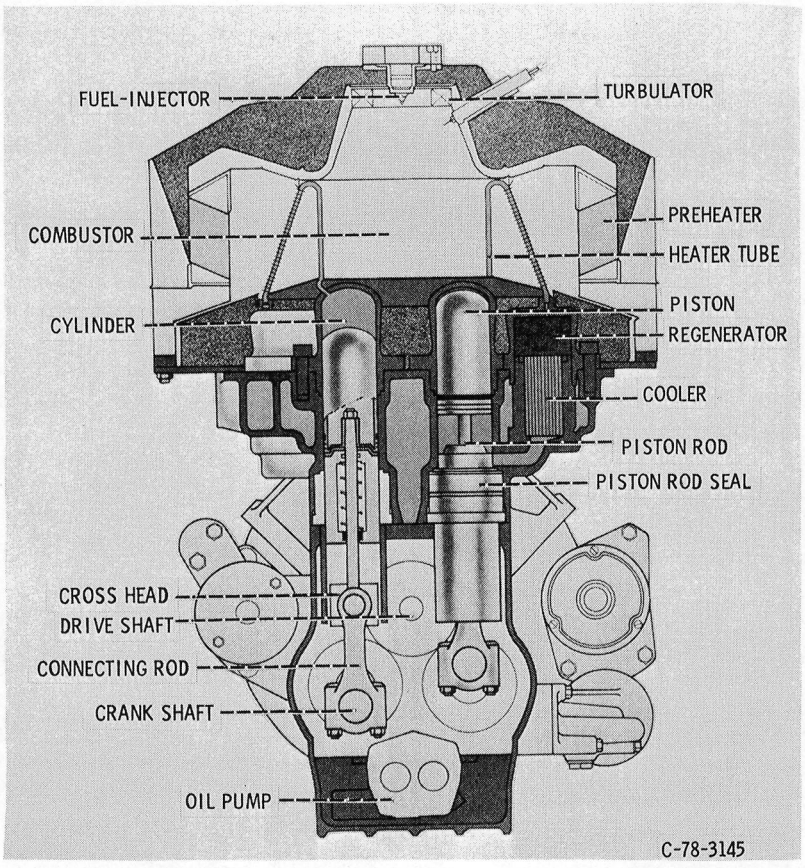

Figure 1. - Schematic representation of automotive Stirling engine.

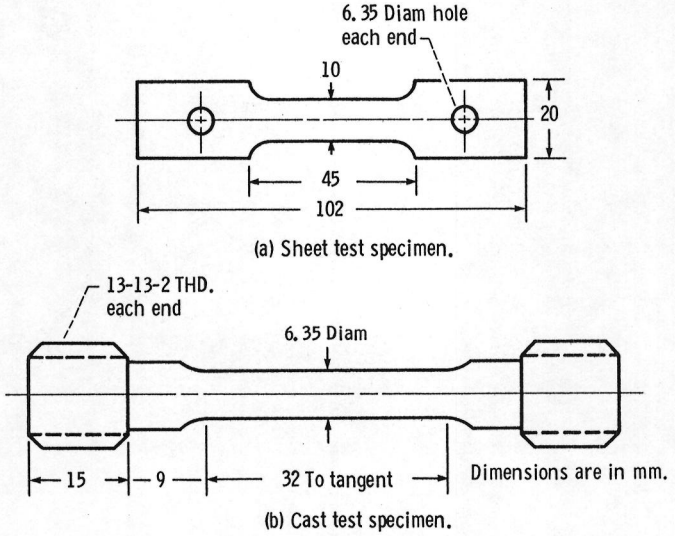

(a) Sheet test specimen.

(b) Cast test specimen.

Figure 2. - Creep rupture specimen design.

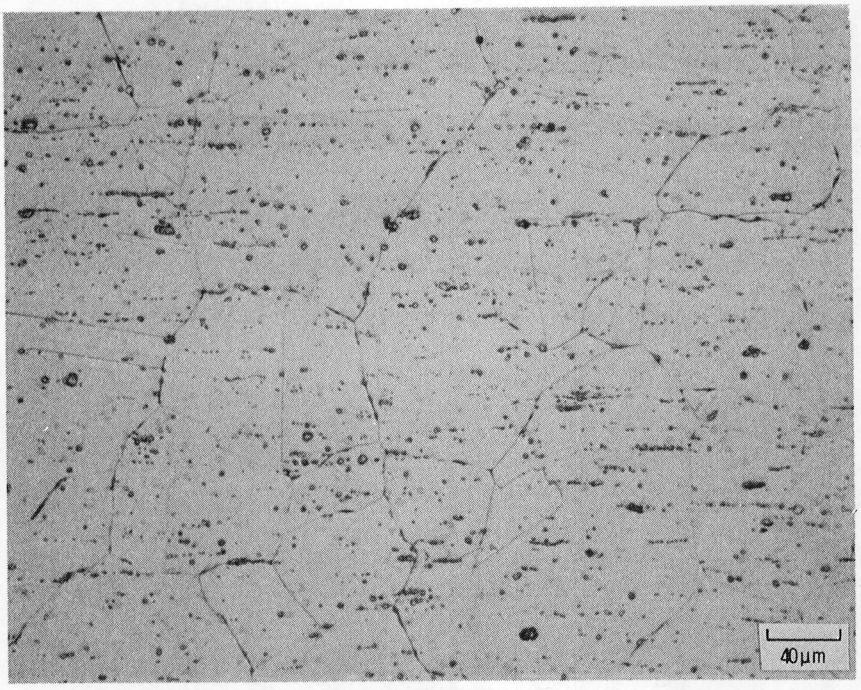

(a) W545

(b) IN718

Figure 3. - Microstructures of unaged candidate heater tube alloys.

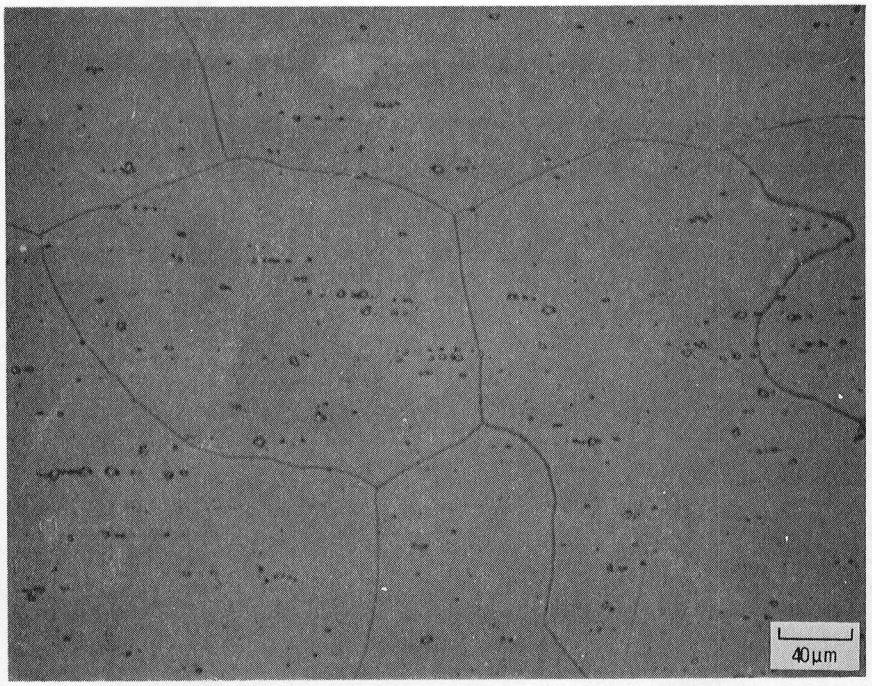

(c) CG-27

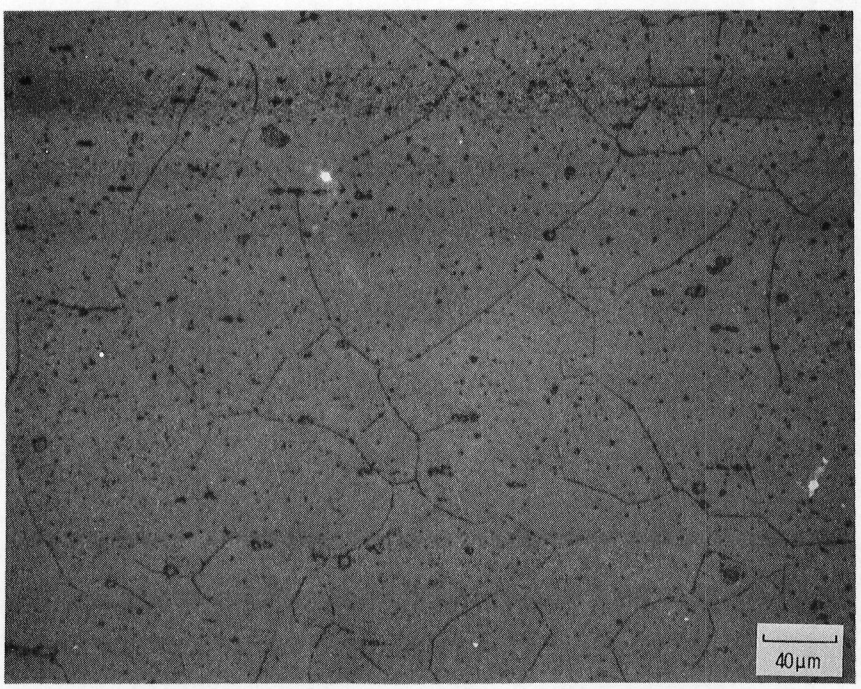

(d) 12RN72

Figure 3. -Continued.

(e) HS-188

Figure 3. - Concluded.

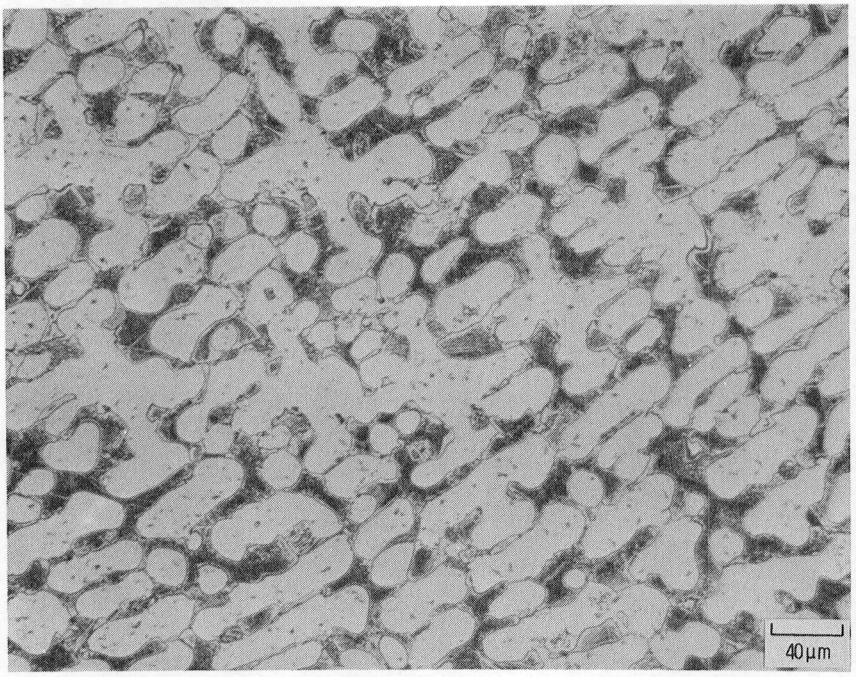

(a) SA-F11

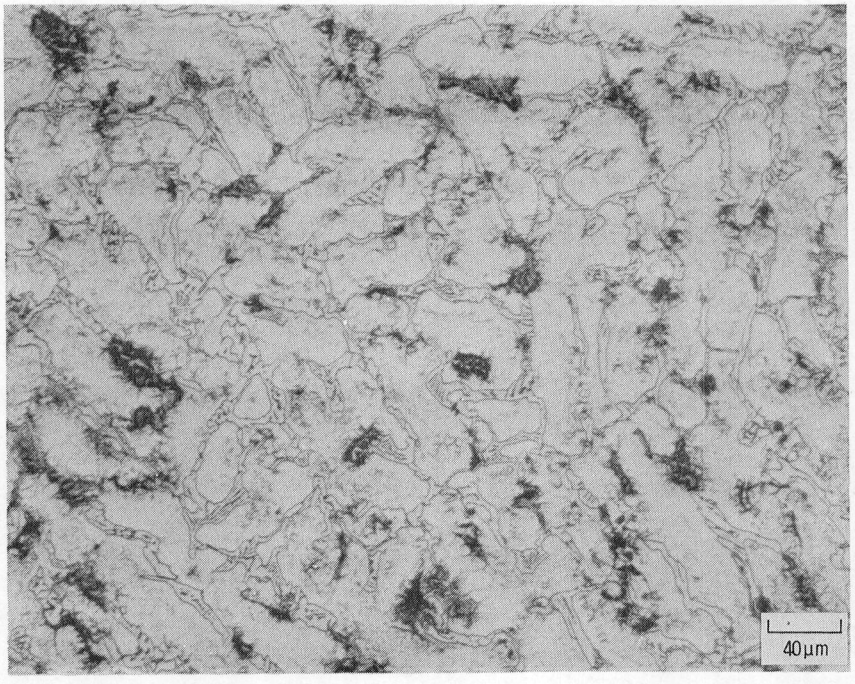

(b) CRM-6D

Figure 4. - Microstructure of unaged candidate cast cylinder and regenerator housing alloys.

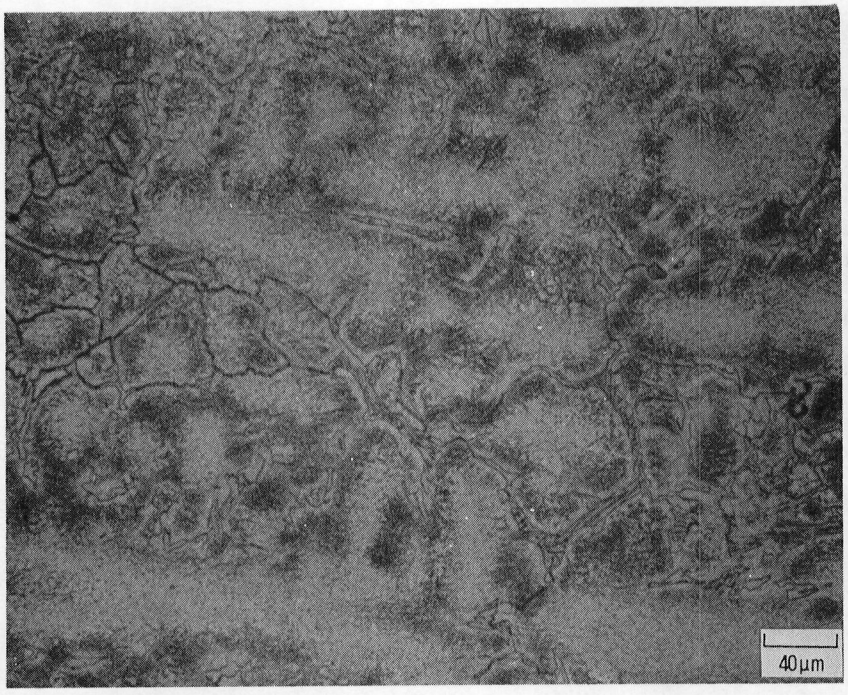

(c) XF-818

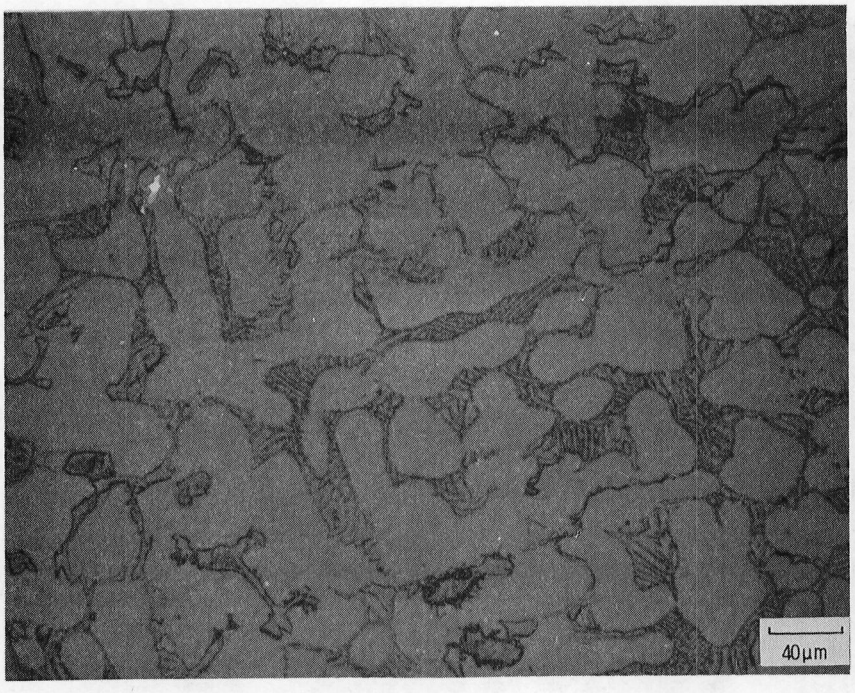

(d) HS-31

Figure 4. - Concluded.

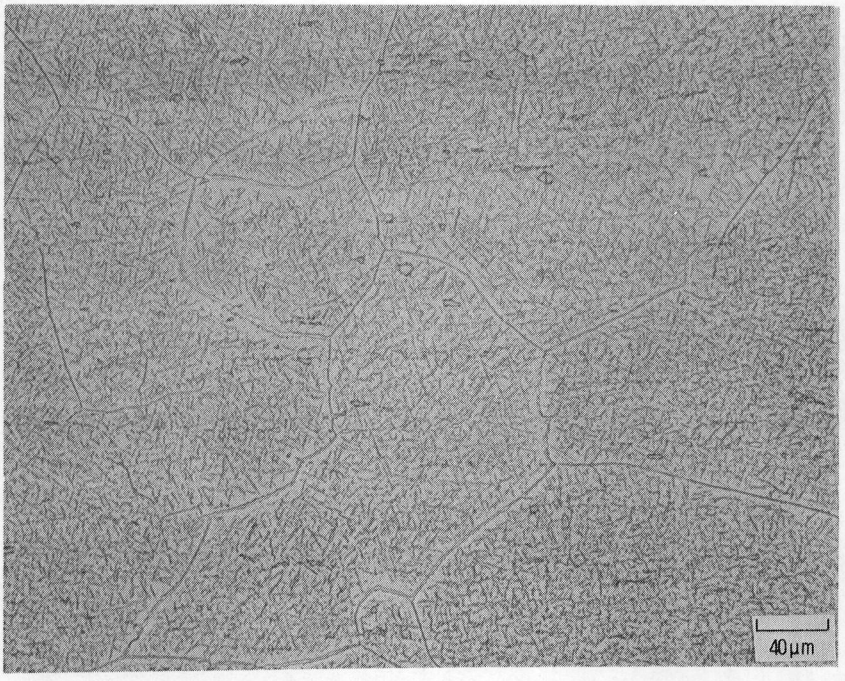

(a) Ar.

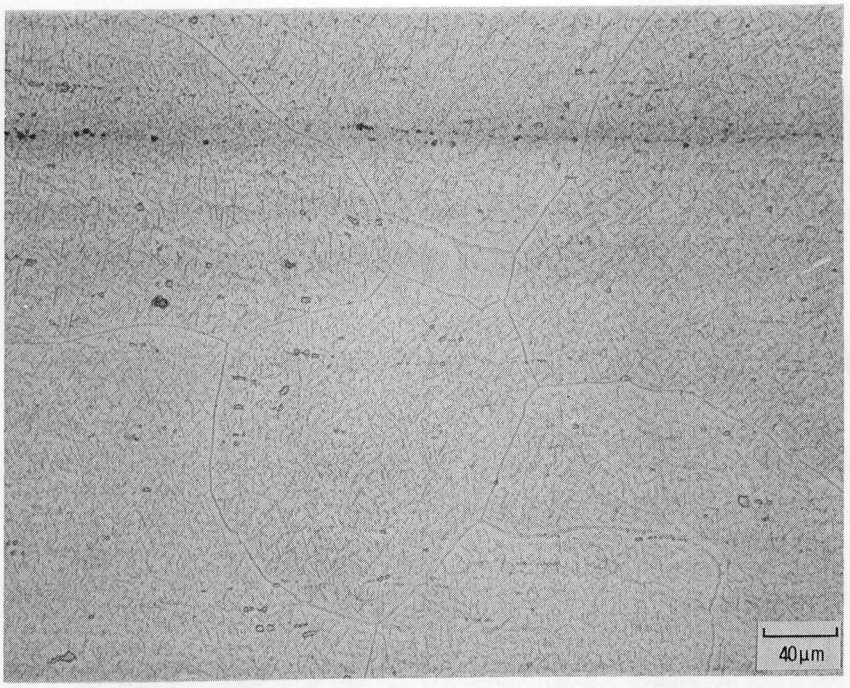

(b) H_2.

Figure 5. - Microstructure of CG-27 alloy after long term (3500 hour) aging at 760° C.

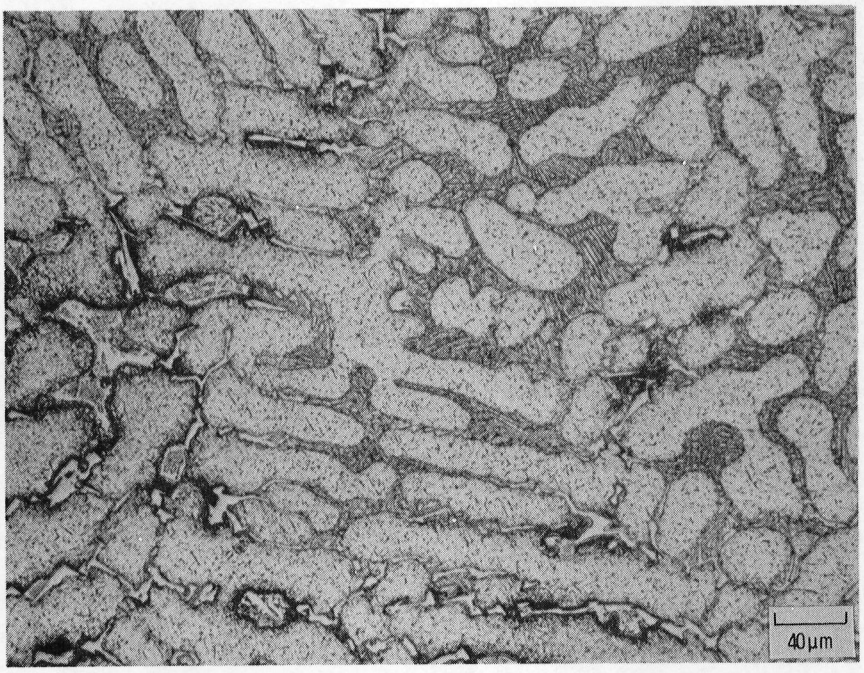

(a) Ar.

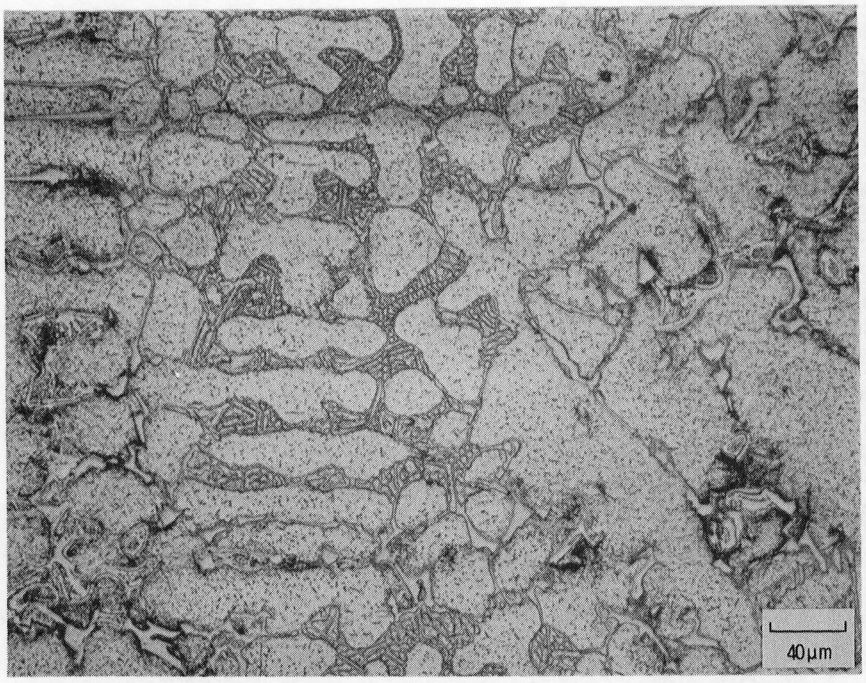

(b) H_2.

Figure 6. - Microstructure of XF-818 alloy after long term (3500 hour) aging at 760° C.

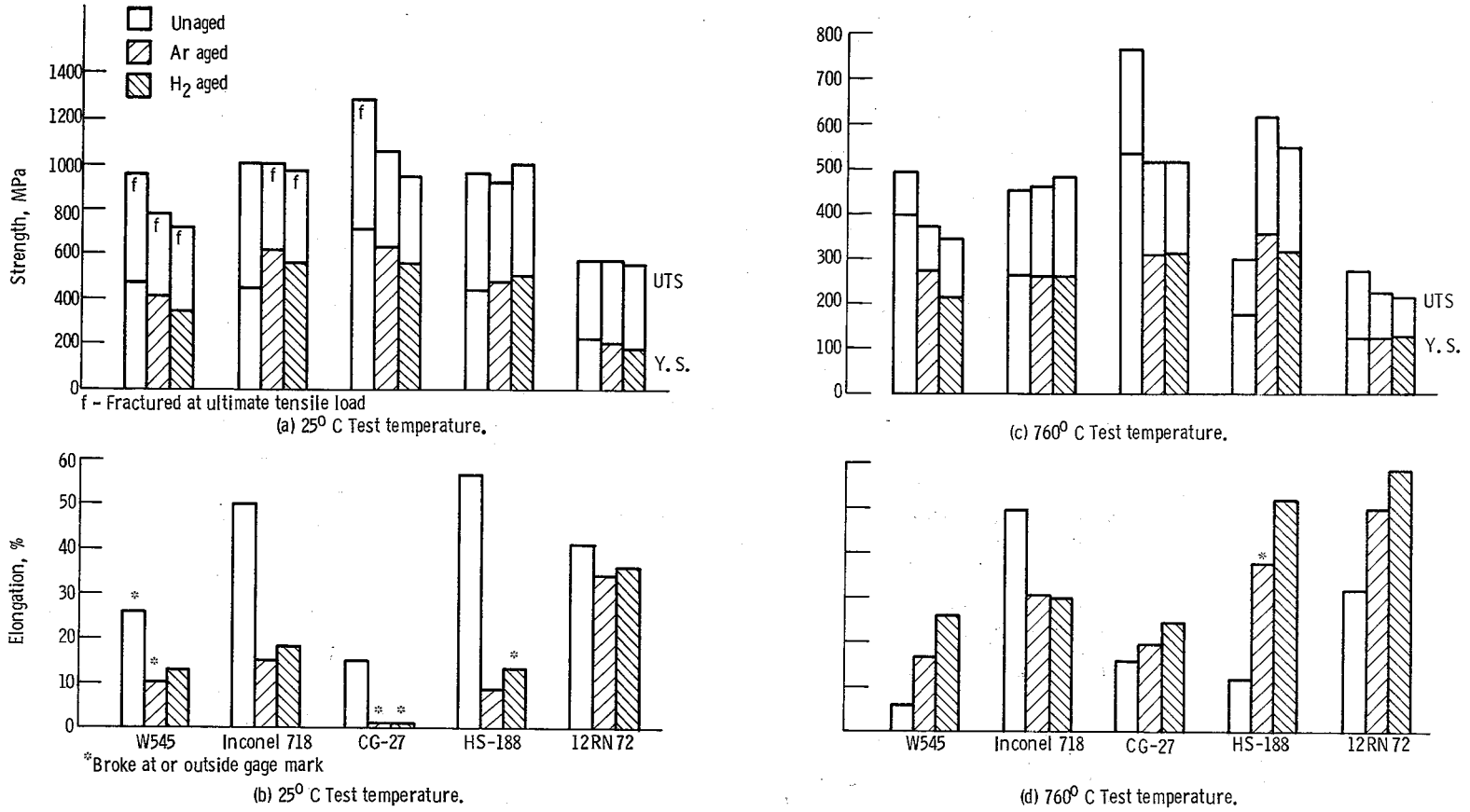

Figure 7. - Tensile properties of candidate heater tube alloys in the unaged, Ar aged and H_2 aged conditions.

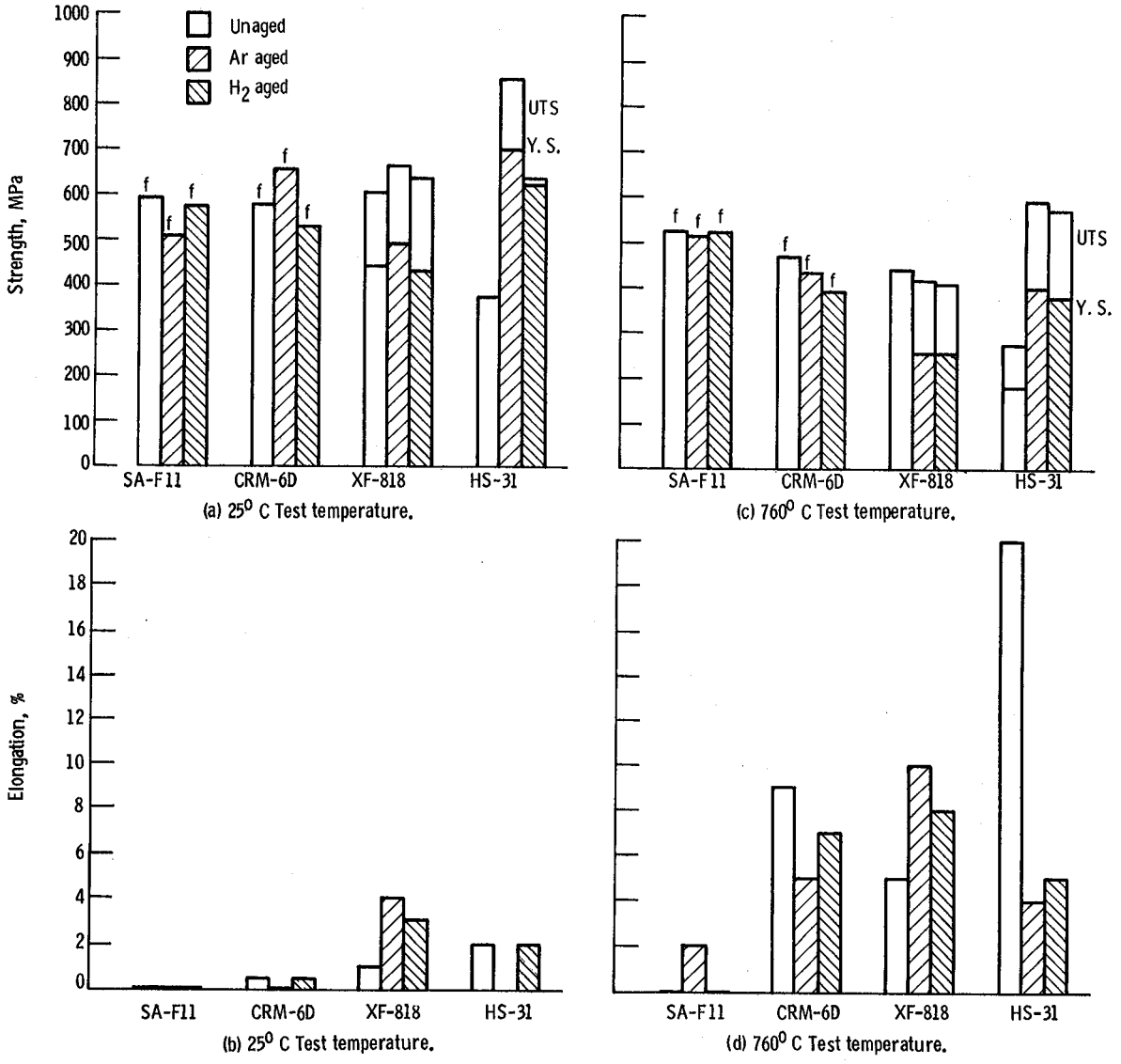

Figure 8. - Tensile properties of candidate cylinder and regenerator housing alloys in the unaged, Ar aged and H_2 aged condition.

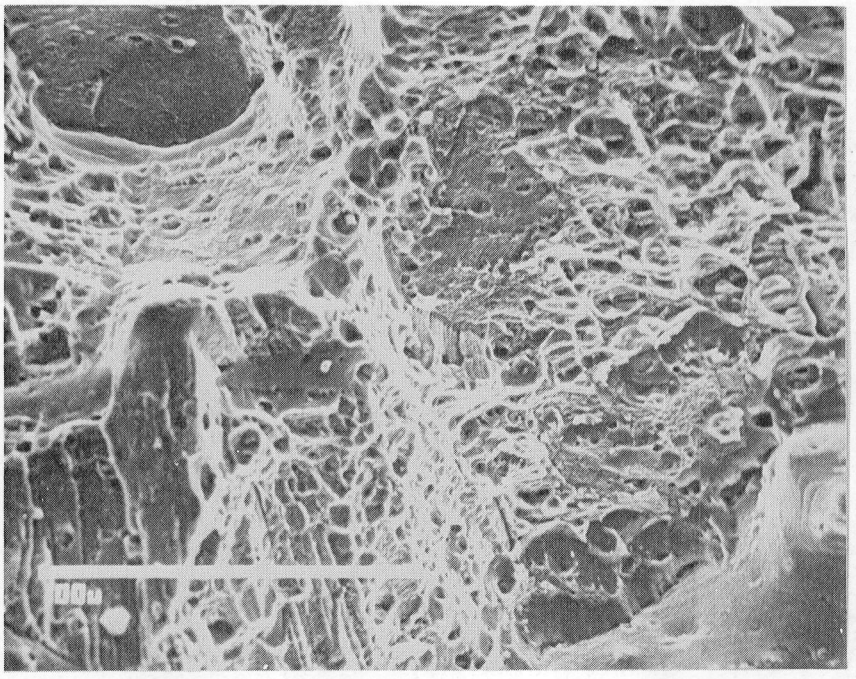

(a) Unaged.

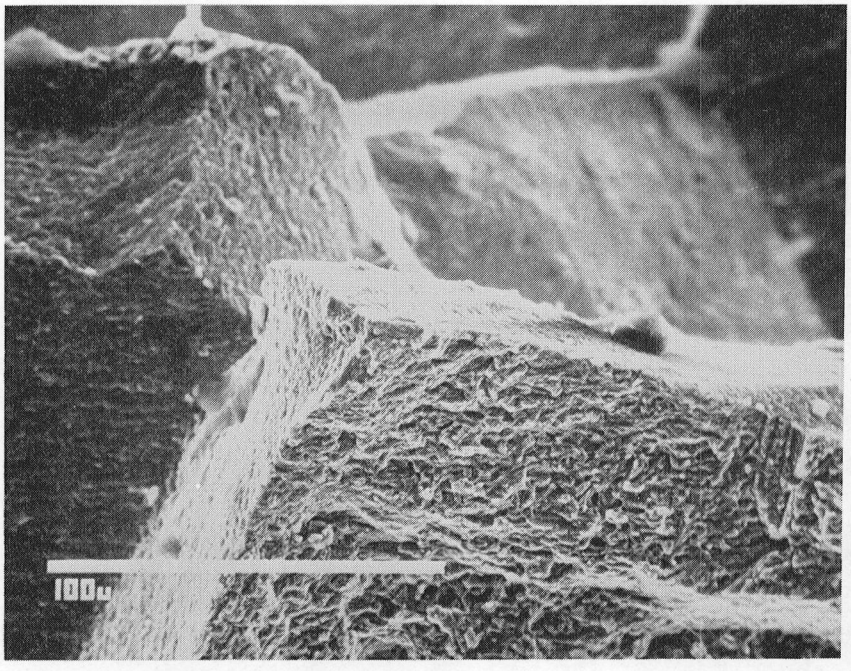

(b) Aged 3500 hr at 760° C in H_2.

Figure 9. - Microfractographs of surface of CG-27 alloy tensile tested at 25° C.

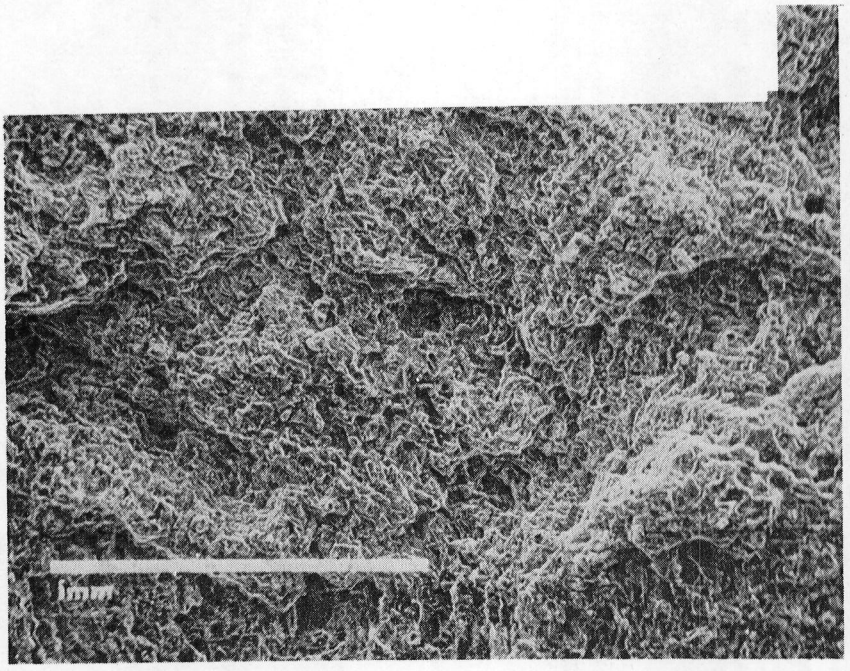

(a) Unaged.

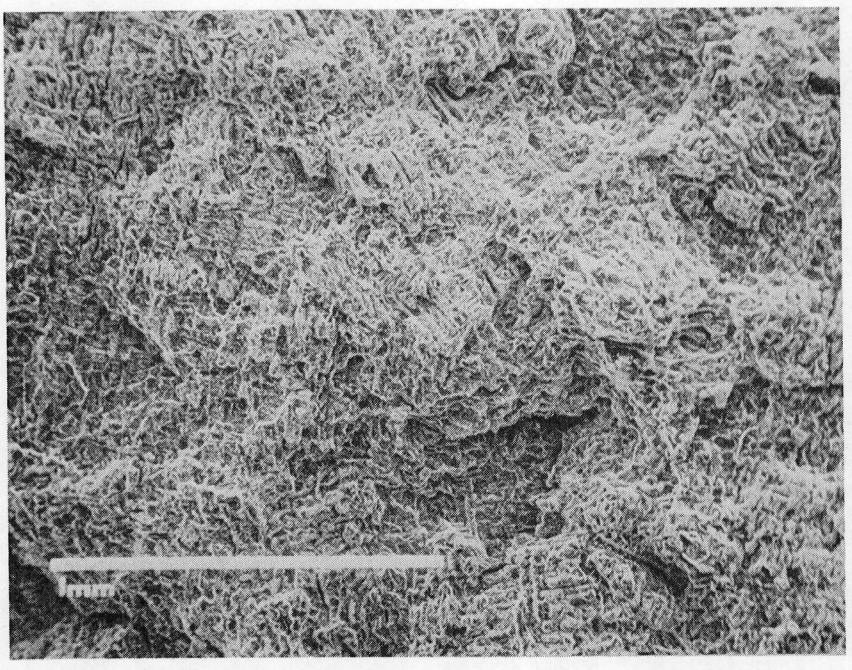

(b) Aged 3500 hr at 760^{0} in H_2.

Figure 10. - Microfractograph of surface of XF-818 alloy tensile tested at 25^{0} C.

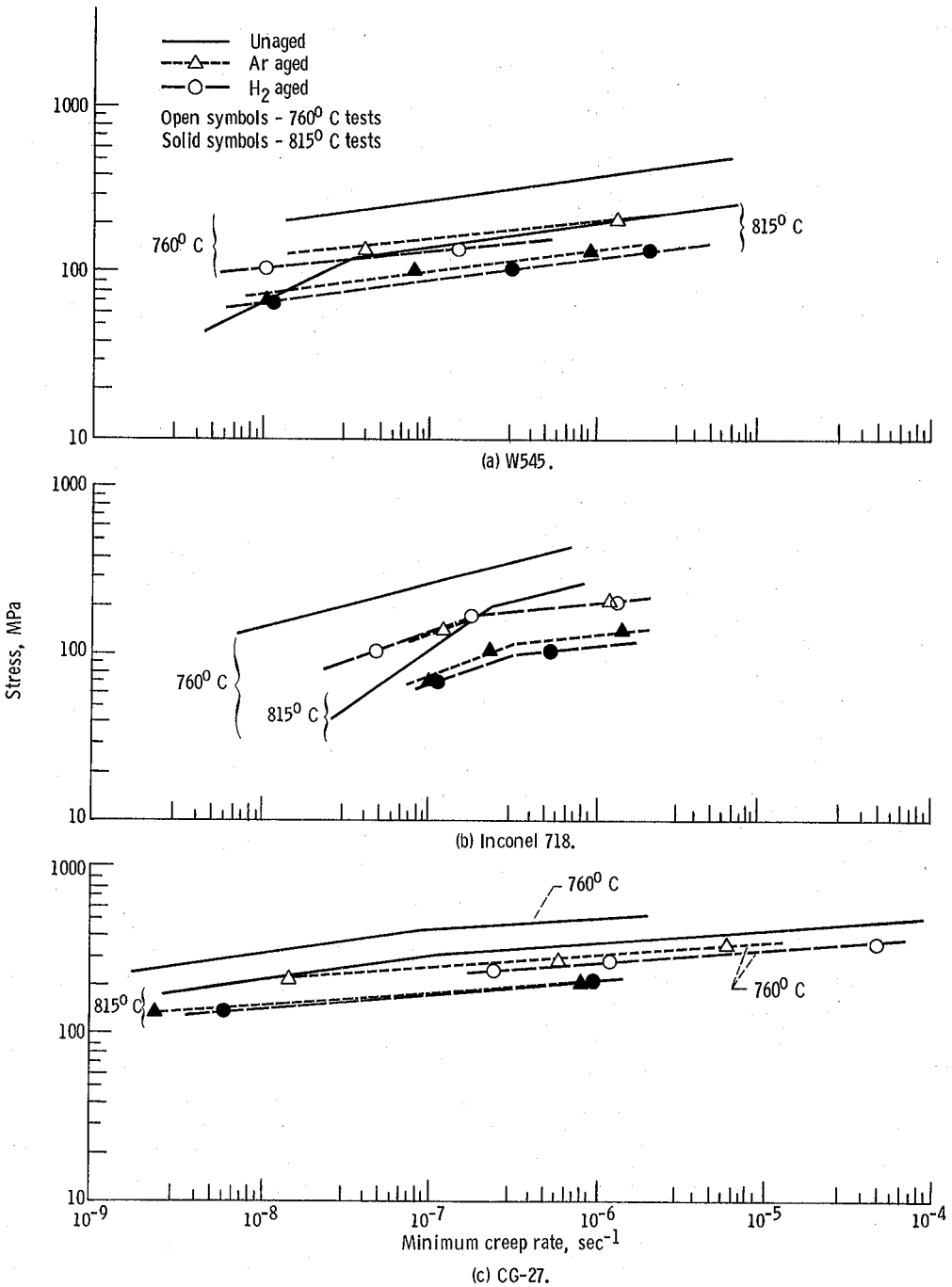

Figure 11. - Minimum creep rates for candidate heater head alloys in the unaged and aged conditions at 760° and 815° C.

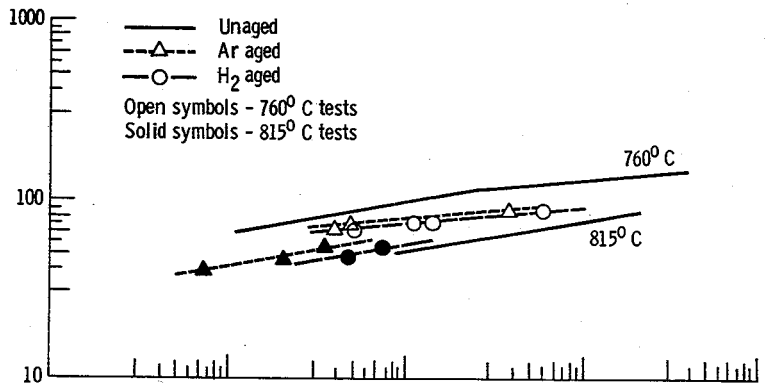

(d) 12RN 72.

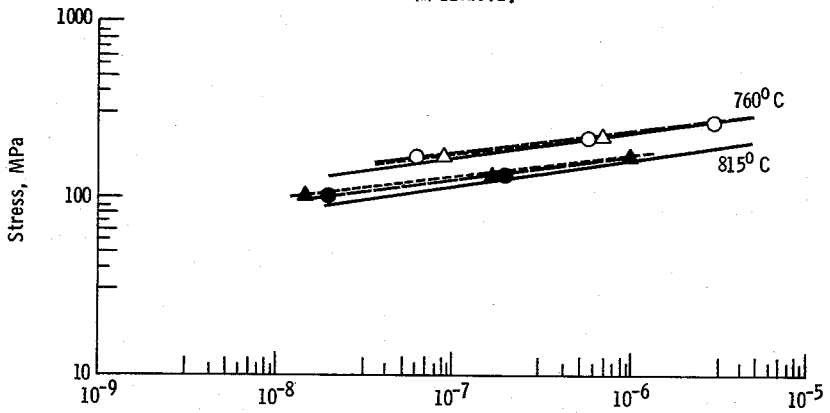

(e) HS-188.

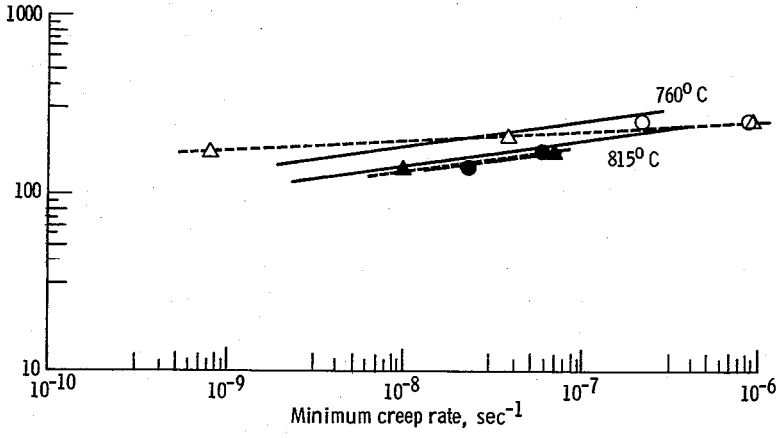

(f) SA-F11

Figure 11. - Continued.

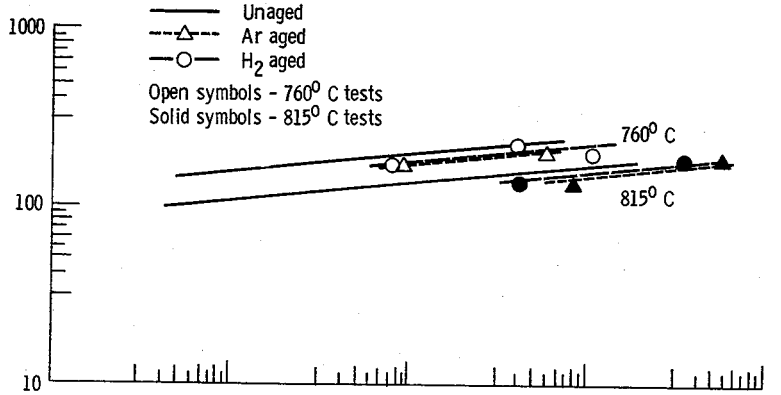

(g) CRM-6D.

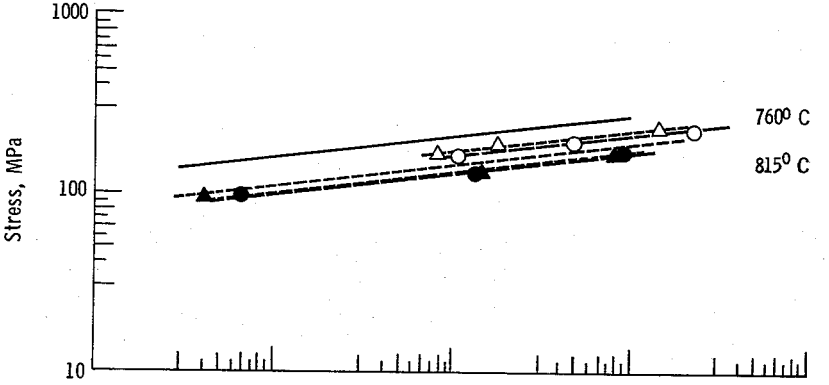

(h) XF-818.

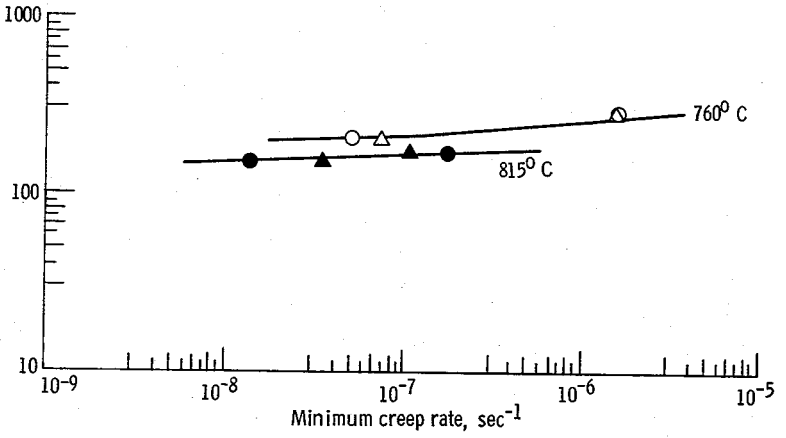

(i) HS-31.

Figure 11. - Concluded.

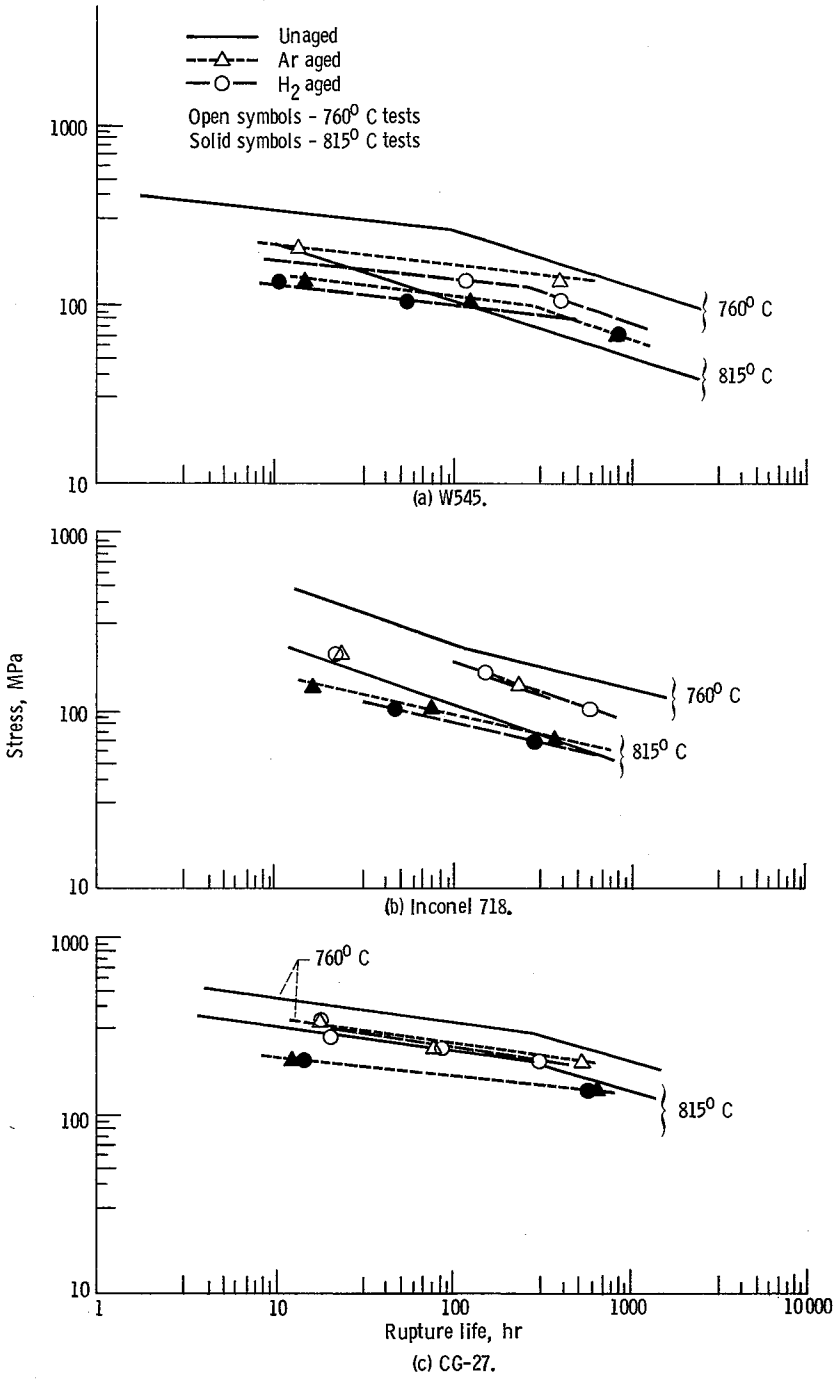

Figure 12. - Rupture lives of candidate heater head alloys in the unaged and aged conditions at 760° and 815° C.

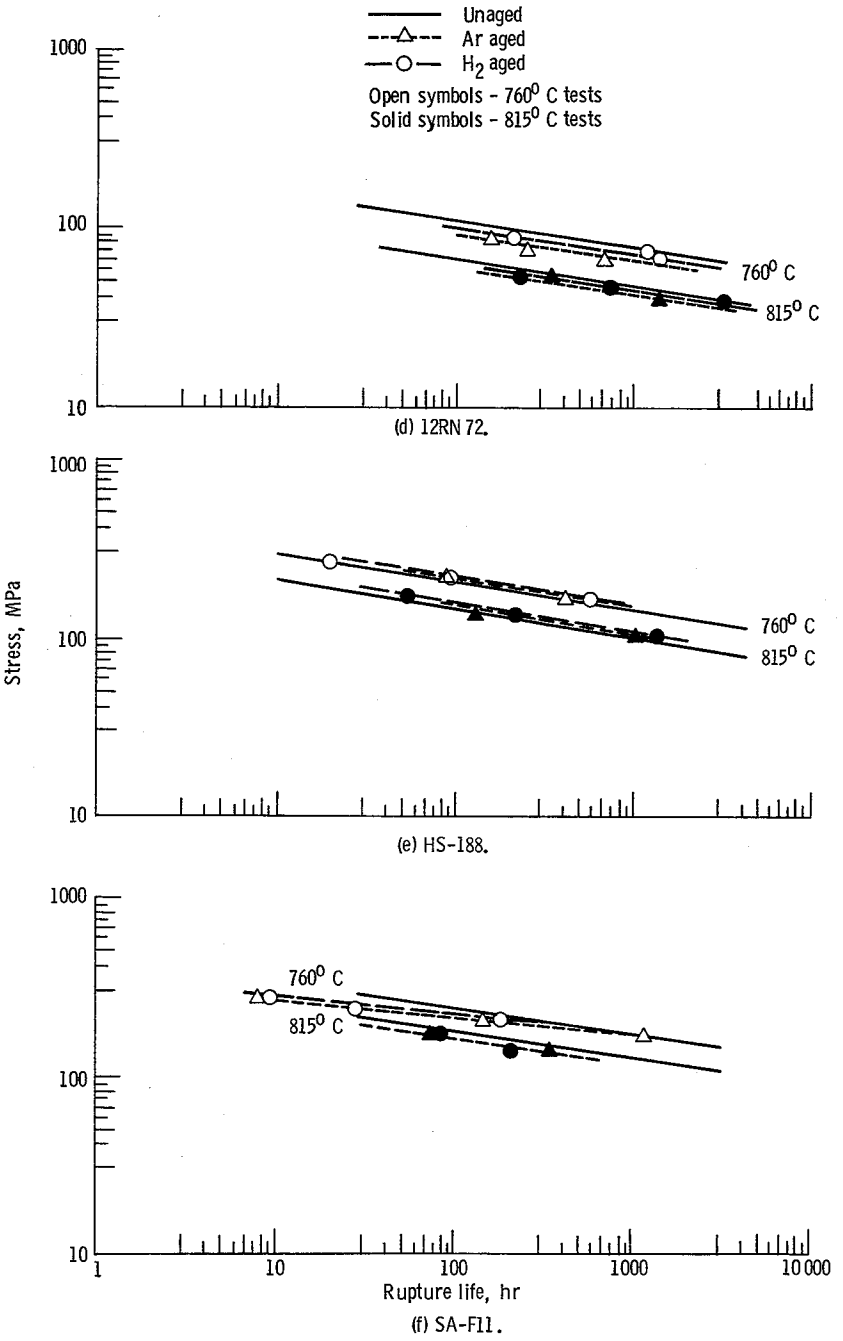

Figure 12. - Continued.

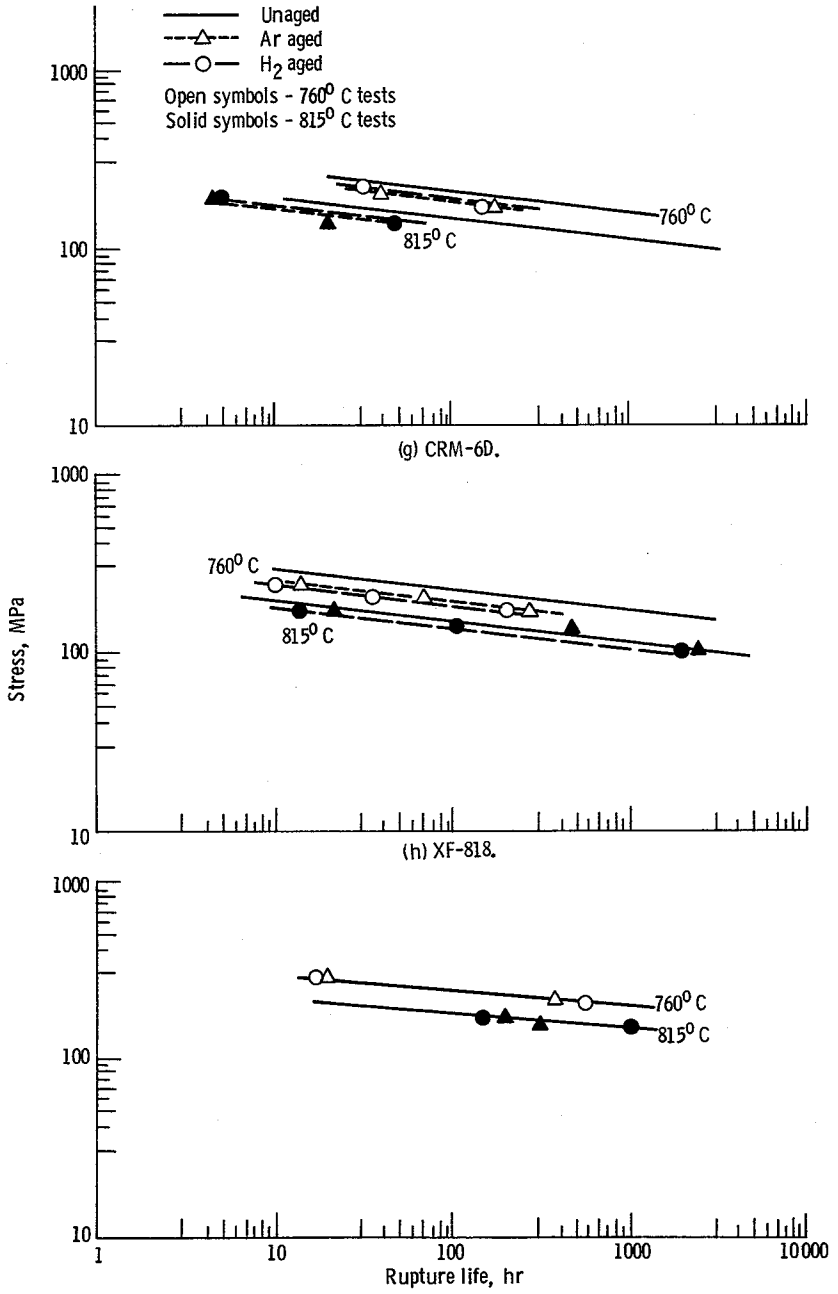

Figure 12. - Concluded.

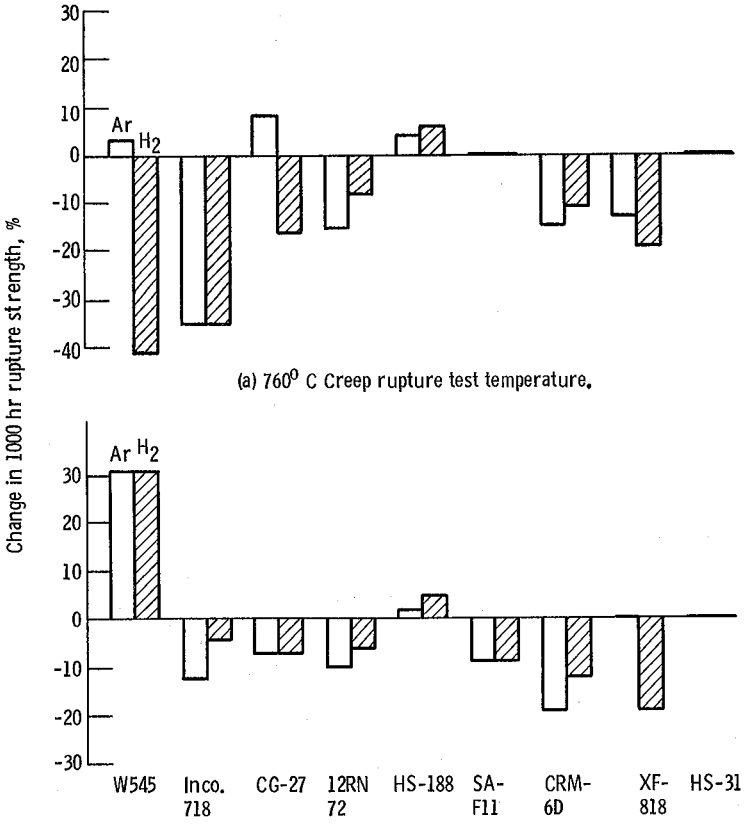

(a) 760° C Creep rupture test temperature.

(b) 815° C Creep rupture test temperature.

Figure 13. - Change in 1000 hr rupture strength of alloys at 760° and 815° C after aging for 3500 hr in argon or hydrogen.

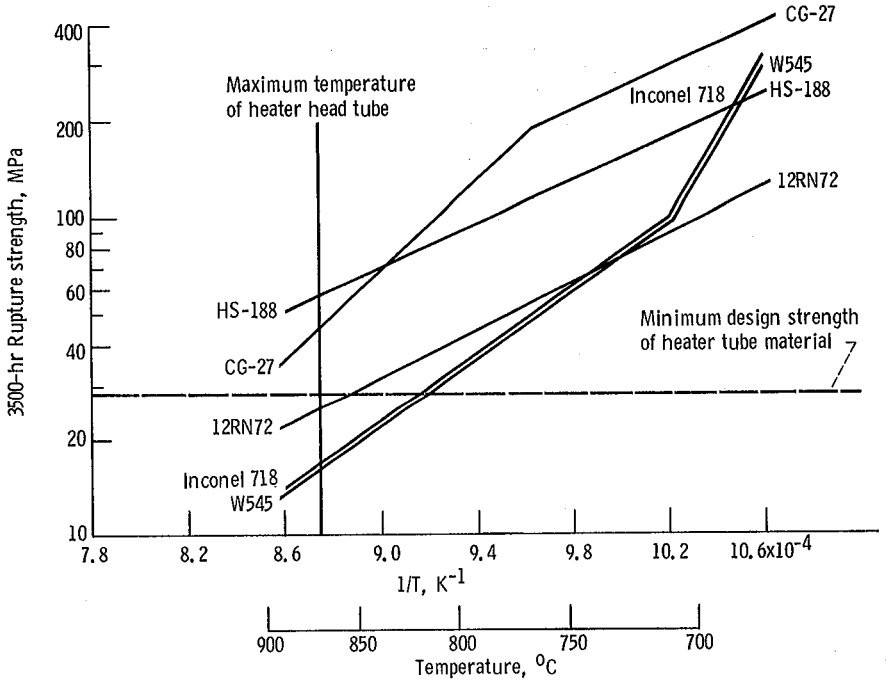

(a) Heater tube alloys.

Figure 14. - The temperature dependency of rupture strength for unaged candidate Stirling engine alloys compared to the MOD. 1A Stirling automotive engine requirements.

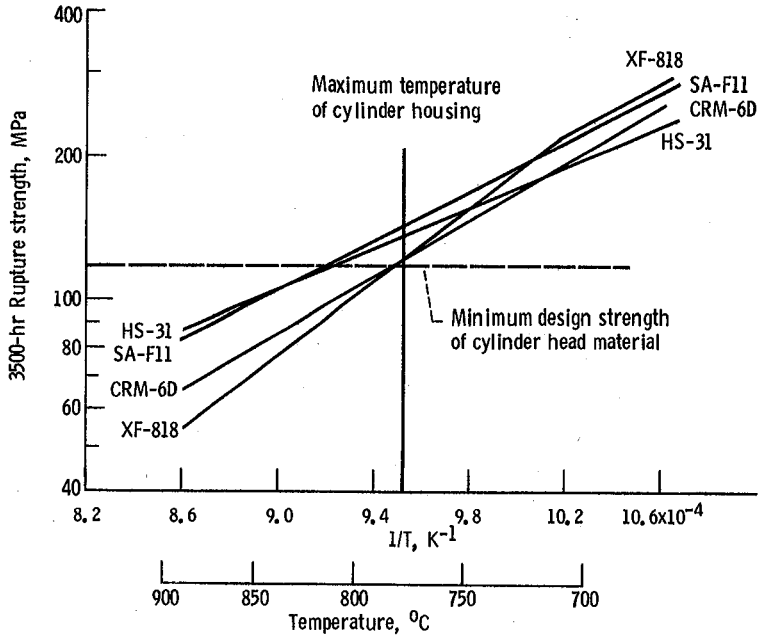

(b) Cylinder head alloys.

Figure 14. - Concluded.

1. Report No.	2. Government Accession No.	3. Recipient's Catalog No.
NASA TM-83676		

4. Title and Subtitle	5. Report Date
Creep-Rupture Behavior of Candidate Stirling Engine Alloys After Long-Term Aging At 760° C in Low-Pressure Hydrogen	May 1984
	6. Performing Organization Code: 778-35-0300
7. Author(s): Robert H. Titran	8. Performing Organization Report No.: E-2124
	10. Work Unit No.
9. Performing Organization Name and Address: National Aeronautics and Space Administration, Lewis Research Center, Cleveland, Ohio 44135	11. Contract or Grant No.
	13. Type of Report and Period Covered: Technical Memorandum
12. Sponsoring Agency Name and Address: U.S. Department of Energy, Office of Vehicle and Engine R&D, Washington, D.C. 20545	14. Sponsoring Agency Code Report No.: DOE/NASA/51040-55

15. Supplementary Notes

Final report. Prepared under Interagency Agreement DE-AI01-77CS51040.

16. Abstract

Nine candidate Stirling automotive engine alloys were aged at 760° C for 3500 hr in low pressure hydrogen or argon to determine the resulting effects on mechanical behavior. Candidate heater head tube alloys were CG-27, W545, 12RN72, INCONEL-718, and HS-188 while candidate cast cylinder-regenerator housing alloys were SA-F11, CRM-6D, XF-818, and HS-31. Aging per se is detrimental to the creep-rupture and tensile strengths of the iron-base alloys. The presence of hydrogen does not significantly contribute to strength degradation. Based on current MOD 1A Stirling engine design criteria of a 55 percent urban - 45 percent highway driving cycle; CG-27 has adequate 3500 hr - 870° C creep-rupture strength and SA-F11, CRM-6D, and XF-818 have adequate 3500 hr - 775° C creep-rupture strength.

17. Key Words (Suggested by Author(s))

Stirling engine
Creep-rupture
Hydrogen
Iron alloys

18. Distribution Statement

Unclassified - unlimited
STAR Category 26
DOE Category UC-96

19. Security Classif. (of this report)	20. Security Classif. (of this page)	21. No. of pages	22. Price*
Unclassified	Unclassified		A02

*For sale by the National Technical Information Service, Springfield, Virginia 22161

National Aeronautics and
Space Administration

Washington, D.C.
20546

Official Business
Penalty for Private Use, $300

SPECIAL FOURTH CLASS MAIL
BOOK

Postage and Fees Paid
National Aeronautics and
Space Administration
NASA-451

NASA

POSTMASTER: If Undeliverable (Section 158
Postal Manual) Do Not Return